5. A review of crop frost damage models and their potential application to cover crops

Mara Gabbrielli[1], Alessia Perego[1], Marco Acutis[1], Luca Bechini[1]

[1]Department of Agricultural and Environmental Sciences-Production, Landscape, Agroenergy, Università degli Studi di Milano, via Celoria 2, 20133 Milano, Italy

Corresponding author: Mara Gabbrielli, mara.gabbrielli@unimi.i

ABSTRACT

Cover crops provide agro-ecological services like erosion control, improvement of soil quality, reduction of nitrate leaching and weed control. Before planting the subsequent cash crop, cover crops need to be terminated with herbicides, mechanically or with the help of frost (winterkill). Winterkill termination is expected to increase its relevance in the next years, especially for organic farming due to limitations in the use of herbicides and for conservation agriculture cropping systems. Termination by frost depends on complex interactions between genotype, development stage and weather conditions. To understand these interactions for management purposes, crop frost damage models, whose review is the purpose of this article, can be very useful. A literature search led to the collection of eight frost damage models, mainly dedicated to winter wheat. Three of these models are described in detail because they appear suited to adaptation to cover crops. Indeed, they explicitly simulate frost tolerance acquisition and loss as influenced by development stage using a crop frost tolerance temperature, whose rate of variation depends on the processes of hardening and dehardening. This tolerance temperature is compared daily with environmental temperature to calculate frost damage to the vegetative organs. The three models, when applied to winter wheat in Canada, Norway and France, have shown good agreement between measured and simulated crop frost tolerance temperature (when declared, the root mean squared error was 2.4 °C). To compare the behaviour of these models, we applied them in two locations with different climatic conditions (temperate climate: Sant'Angelo Lodigiano, Italy, and continental climate: Saskaatoon, Canada) with respect to frost tolerance acquisition. This comparison revealed that the three models provide different simulated dates for the frost damage event in the continental site, while they are more similar in the temperate site. In

conclusion, we have shown that the reviewed models are potentially suitable for simulating cover crop frost damage.

HIGHLIGHTS

- Frost termination is very important for cover crops and needs to be simulated with crop models.
- Lacking a cover crop frost damage model, we review eight models simulating damage of cash crops, namely cereals.
- Three of these models are also applicable to cover crops and are described in more detail.
- The simulated crop frost tolerance temperature decreases and increases with hardening and dehardening, respectively.
- This tolerance temperature is compared with environmental temperature to calculate frost damage to the crop.

KEYWORDS

Development stage, Frost tolerance, Hardening, Lethal temperature, Termination, Winter wheat, Winterkill.

5.1 INTRODUCTION

A cover crop is included in the annual rotation in the fallow period between the harvest of a cash crop and the sowing of the following one. During this period, without the use of a cover crop, the soil would be bare causing several problems such as nitrate leaching and soil erosion (Justes, 2017). Cover crop cultivation puts into effect one of the principles of conservation agriculture that consists of maintaining a permanent soil cover. Indeed, cover crops are not planted with the purpose of being harvested, and therefore generating income, but to avoid the occurrence of a bare soil period in the crop rotation and provide agro-ecological services. Cover crops exert several agro-ecological functions that provide agronomic benefits such as: reduction of nitrate leaching (Tonitto et al., 2006), soil erosion, weed growth (Osipitan et al., 2018), and pest/pathogen pressure; nitrogen provision for the following cash crop; increase of soil organic matter (Poeplau and Don, 2015), improvement of soil physical properties and increase of agro-ecosystem biodiversity (Justes, 2017). Therefore, cover crop cultivation is becoming increasingly relevant for conservation and conventional cropping systems. Cover crop management consists of two main operations (sowing and termination), and their date and operational conditions strongly affect the agro-ecological services provided by the cover crop (Justes, 2017).

This review focuses on termination, which is the process that kills the cover crop and prevents its growth continuing during the cash crop growing season. In most cases, cover crops are terminated before or during

soil preparation for the sowing of the following cash crop. Cover crop termination methods depend on the species of cover crop, its development stage and environmental conditions (rainfall and temperature in particular). Cover crop termination can be carried out chemically (using a herbicide), mechanically by mowing, harrowing or rolling (Creamer and Dabney, 2002), or be caused by winter low temperatures (Labreuche and Bodilis, 2010; Labreuche and Collet, 2010). Cover crop winterkill is particularly convenient because it saves cultivation costs (fuel, manpower and chemicals), avoids soil disturbance caused by tractor passes, and avoids using herbicides that may be harmful to humans and the environment. Therefore, cover crop winterkill is very important in cultivation systems where herbicide applications are restricted or forbidden (e.g., organic farming), or where mechanical termination methods are limited (e.g., conservation agriculture). The possibility for a plant to be killed by frost depends on genotype, development stage and weather conditions (Janská et al., 2010). Sowing date is therefore important because it determines, together with temperature and photoperiod, the development stage reached at the moment of frost. In general, plant susceptibility to winterkill is lower during the earlier phenological stages and increases over time (Ambroise et al., 2020).

Experimental trials may fail in exploring a wide range of pedoclimatic conditions and agronomic management practices. Instead, the effect of the complex interactions between genotype, development stage and weather on cover crop winterkill can be effectively represented with mechanistic dynamic simulation models. To the best of our knowledge, existing cropping system models do not simulate the process of cover crop damage by winter frosts. An option to improve current models is to adapt to cover crops the modules available for the simulation of frost damage on annual crops like cereals (e.g. Byrns et al. 2020).

Therefore, the aim of this work is to review and compare existing frost damage modules incorporated in cropping systems models, to provide a basis for the development of a cover crop damage simulation model. We first describe the physiological bases of frost damage and frost tolerance of plants. We then describe the literature search aimed at the identification of the existing models for cereal and dicotyledonous crops. Three of the models found in literature are then described in detail because they look particularly adequate for

adaptation to cover crops. Finally, the outputs of the three selected models are presented for test cases in different sites.

5.2 PHYSIOLOGICAL BASES OF FROST DAMAGE AND FROST TOLERANCE

Cold damage occurs when plants are exposed to low temperatures which lay outside the optimal temperature range for growth and development, but greater than 0°C, i.e. not low enough to lead to ice formation. Cold damage gives rise to growth reduction, leaf damage and withering due to root cooling (Smallwood and Bowles, 2002). Low temperatures reduce cell membrane fluidity and therefore cause membrane protein malfunctioning, and, as the final result, the inhibition of several biochemical processes such as energy transduction, solutes transport and H+-ATPase activity (Muzi et al., 2016). Frost damage, on the contrary, occurs as a result of the exposure to sub-zero temperatures and leads to extra-cellular and then to intra-cellular ice crystal formation. Extra-cellular ice crystals cause cell membrane damage due to cell dehydration, since ice formation reduces apoplast water potential so that water can move from the symplast (having higher water potential) to the apoplast. Tissue damage due to extra-cellular ice crystals is reversible as long as the plant is tolerant and the exposure time to freezing temperatures is short. Later on, if exposure to frost continues, ice crystals form inside the cell (symplast), destroying both cell membranes and cellular organelles leading to cellular death. Intra-cellular ice crystal formation results in lethal damage to the plant (Beck et al., 2004).

Plants can be divided into four frost sensitivity categories: tender; slightly hardy; moderately hardy; and very hardy (Levitt, 1980). Tender plants are those that do not develop systems of avoidance of intra-cellular freezing, while slightly hardy plants are sensitive to freezing down to about -5 °C. Moderately hardy plants include those that are able to accumulate sufficient solutes to avoid dehydration damage, thus resisting freeze injury at temperatures as low as -10 °C. Very hardy plants are the ones able to avoid frost damage even at temperatures lower than -10 °C through the avoidance of intracellular freezing as well as cell desiccation (Snyder and Melo-Abreu, 2005).

The duration of freezing temperature plays a key role in determining the extent of frost damage (Muzi et al., 2016). During their evolution, most temperate plant species have developed a certain degree of frost

tolerance depending on the combination of the minimum temperature at which they have been exposed and the length of exposure to cold stress itself (Janská et al., 2010). The adaptation of herbaceous crops to the evolution of cold temperatures over time involved both physiological permanent morphological structural changes and several other phenological and physiological responses induced by low temperatures. The permanent changes, evolved mainly by C3 herbaceous species, consist of height and leaf area reduction, sugar storage in underground tissues, rapid mobilisation of stored reserves (Guy, 1999) and meristematic tissue position and protection adjustments. The timing of phenological and physiological responses induced by low temperature stress is subject to strict genetic control (Guy, 1999). Therefore, the variability of tolerance expressed by a plant is determined firstly by genotype, and then by plant phenological stage and physiological conditions at the time of exposure (Janská et al., 2010). Plant organs differ in their low-temperature tolerance potential: the crown, the meristematic tissue responsible for shoot and root production, has been found to be less sensitive than roots (McKersie and Leshem, 1994).

According to Janská et al. (2010), plants respond to low-temperature stress adopting two strategies: (i) stress avoidance, by means of protection of sensitive tissues and supercooling; (ii) stress tolerance, by means of cold acclimation. The meristematic tissues are protected from freezing by coverage with leaves or belowground placement, while supercooling consists of inhibiting the formation of ice nucleators (molecules around which ice crystals are formed). Plant acclimation to low-temperature stress is known as hardening and it is achieved through exposure to low temperatures (Fowler et al., 1999). The hardening process allows plants to increase their subsequent frost tolerance and involves several transcriptional and physiological adjustments such as cold-regulated genes activation, membrane fluidity alterations, photosynthesis downstream regulation, osmoprotectant compound accumulation, antioxidant system stimulation (Hassan et al., 2021). Fowler et al. (1999) underline that, since cold acclimation of winter cereals is a cumulative process (that begins with the exposure to low temperatures and that can undergo interruptions, inversions and re-starts), it is the series of temperatures to which the plant is exposed that determines both the frost tolerance entity and its maintenance, and the eventual subsequent degree of frost damage.

5.3 METHODOLOGY

We performed a literature search with the aim of finding crop simulation models with algorithms for frost damage simulation. The literature search was carried out on Scopus (http://www.scopus.com) and Web of Science (http://www.webofknowledge.com) with the following query:

(freezing tolerance OR frost tolerance OR cold tolerance OR low temperature tolerance OR frost resistance OR cold resistance OR low temperature resistance OR winter survival OR low temperatures survival OR frost damage OR frost injury OR freezing damage OR freezing injury OR frost killing OR winterkill OR winterkill risk OR winter damage) AND (model OR modelling OR simulation OR simulating OR estimate OR estimating OR assessment OR evaluation) AND (herbaceous crop OR herbaceous plant OR crop OR cereal).

As a result of the search we collected 508 papers. After screening, we selected 11 frost damage models and a review (Barlow et al., 2015) regarding the modelling of extreme weather events on wheat production. The analysis of the 11 papers indicated that crop simulation models represent frost damage by means of different strategies; leading to various levels of detail for damage representation. Among the models emerging from the literature search, we selected those with the following characteristics that make them suitable for application to cover crops. Firstly, since frost tolerance depends on development stage, the models need to estimate frost tolerance and damage as influenced by crop phenological stage. Secondly, since cover crops are not grown to produce fruits and seeds, but are normally terminated at or before flowering, the models need to simulate the damage of vegetative organs. Therefore, the models that evaluate only frost damage on reproductive organs or the ones that assess only frost effects on crop yield were excluded from this review. The selected models will allow, after calibration, the evaluation of cover crop species and sowing date effects on winterkill termination efficiency, defined as the percentage of plants that do not overwinter.

The eight models selected, which are reviewed below, simulate frost damage and the main physiological processes involved in low temperature acclimation (cold hardening, from now on named ‘hardening’; dehardening; and other abiotic stresses affecting acclimation).

5.4 REVIEW OF FROST DAMAGE MODELS

5.4.1 PRESENTATION OF THE SELECTED MODELS

We present here a list of the selected frost damage models, while a brief model description can be found in Table 1: FROSTOL (Bergjord et al., 2008); winter survival model (Byrns et al., 2020); model proposed by Lecomte et al. (2003); ALFACOLD (Kanneganti et al., 1998); CERES-Wheat (Ritchie, 1991); EPIC (Sharpley and Williams, 1990); APSIM-Wheat (Zheng et al., 2015); and STICS (Brisson et al., 2009). The first three models were originally designed for winter wheat (*Triticum aestivum* L.), ALFACOLD is dedicated to alfalfa (*Medicago sativa* L.), while the other cropping system models simulate several different crops.

FROSTOL, the winter survival model by Byrns et al. (2020) and ALFACOLD use soil temperature in the crown region to assess cold hardening and dehardening rates as well as the occurrence of winterkill events, since it is reported that in most climates crop regrowth after overwintering is determined by the surviving tissues located in the crown region itself (Fowler et al., 1999). FROSTOL (Bergjord et al., 2008) and the winter survival model by (Byrns et al., 2020) were both designed to evaluate winter wheat survival during winter. FROSTOL implements some equations from the first version of the winter survival model by Byrns et al. (2020) which, in turn, is the latest version of the model proposed by Fowler et al. (1999) and (2014).

ALFACOLD ("alfalfa model for yield calculation in cold climates", Kanneganti et al. 1998) integrates frost tolerance in an existing model (ALSIM) used for alfalfa forage yield estimation. ALFACOLD estimates soil temperature in the crown region by means of Ritchie's model (Ritchie, 1991). For freezing injury estimation ALFACOLD adopts a similar approach to the one used by Ritchie (1991) for winter wheat.

The model proposed by Lecomte et al. (2003) predicts the evolution of frost resistance of winter wheat. However, unlike FROSTOL and the model by Byrns et al. (2020), whose experimental basis is an artificial frost hardiness test (in which plants are transferred to a controlled-temperature environment to measure their frost tolerance), Lecomte et al. (2003) characterized frost hardiness under natural conditions thanks to an experimental system of rolling greenhouses. This system, which is located in Chaux-des-Prés (Jura Mountains, France), is maintained by INRA since 1950 and is used to evaluate the frost hardiness of all new cereal

cultivars registered in France. This model includes several hypotheses about maximal frost resistance at the coleoptile stage (T_{RX2}) value, phenological stages for the increase of the maximal frost resistance, and hardening rate. The combination of these hypotheses (2 equations to calculate hardening rate × 2 T_{RX2} thresholds × 6 leaf stage ranges) led to the development of 24 different modelling solutions.

CERES-Wheat (Crop Estimation through Resource and Environment Synthesis) was developed to simulate winter or spring wheat growth and development (Ritchie and Otter, 1985), and is now implemented as an individual crop module in DSSAT (Decision Support System for Agrotechnology Transfer). The submodel of low temperatures acclimation and survival (Ritchie, 1991) utilizes principles and information for hardening and dehardening acquired from previous artificial freezing experiments (Gusta and Fowler, 1976) with five winter wheat cultivars and a winter rye cultivar.

5.4.2 SIMILARITIES OF THE SELECTED MODELS

FROSTOL (Figure 1 and Table A1) and the winter survival model (Figure 2 and Table A2) (Byrns et al., 2020) both express frost tolerance as the "lethal temperature 50" (T_{L50}, °C), which is defined as the temperature at which 50% of the plants are killed in an artificial freeze test (Bergjord et al., 2008). In both models the death of the plants occurs when the average daily soil temperature at crown level drops below the lethal temperature T_{L50}.

Lecomte et al. (2003) estimate the crop frost resistance on day *d* (T_R, °C) which is defined as the temperature below which the first leaf damage can occur (Figure 3 and Table A3). Similarly, ALFACOLD quantifies the state of crop cold tolerance using *CTT* (Cold Tolerance Temperature, °C) which corresponds to the subzero temperature that a crop can tolerate without being killed. ALFACOLD uses a crop death coefficient to estimate plant death to due frost damage, while in the model by Lecomte et al. (2003) frost damage occurs when the daily minimum air temperature is equal or drops below the crop frost resistance, T_R.

Finally, a common modeling approach is adopted in CERES-Wheat, EPIC, APSIM and STICS. In these four models, a crop characteristic (like biomass, leaf area index or crop density) is modified daily by a stress factor

that represents the damage by frost. This stress factor is not treated in these models as a state variable but it is calculated at each time step without reference to the value of the previous time step. In all models, the state variable or the stress index representing frost crop resistance is calculated starting from sowing with a daily time step.

We will describe only the three models that fulfil the criteria presented in paragraph 3 (tolerance simulated according to the development stage; damage simulated also for non-reproductive organs): FROSTOL, the winter survival model (Byrns et al., 2020) and the model proposed by Lecomte et al. (2003). For these three models, common symbols were used to describe variables and parameters that have the same meaning (the common symbols employed in this review and the original model symbols are reported in the supplementary material, Table S1). The default values of model parameters are reported respectively in Table A1 (FROSTOL), A2 (model by Byrns et al., 2020) and A3 (model by Lecomte et al., 2003). Of course, these parameters need to be adjusted to apply the models at different cultivars or species. The other five models are described in the supplementary material.

5.4.3 THE THREE MODELS IN DETAIL

5.4.3.1 FROSTOL MODEL

The initial value of the state variable T_{L50} corresponds to the "lethal temperature 50" of an unacclimated crop. In FROSTOL this value (T_{L50i}, °C), Eq.1, depends on the maximum frost tolerance of the cultivar of interest (T_{L50c}, °C) which has been established through a controlled-freeze test of cold hardiness performed by Bergjord et al. (2008).

$$T_{L50i} = -0.6 + 0.142 \cdot T_{L50c} \quad [1]$$

The state variable T_{L50} ranges between T_{L50i} (upper limit) and T_{L50c} (lower limit). In FROSTOL (Bergjord et al., 2008) the rate variable that simulates the daily change of T_{L50} is composed of four equations describing two physiological processes (rT_H, hardening, and rT_D, dehardening) and two stress responses (rT_R, respiration under a snow cover stress, and rT_S, low temperature stress) involved in the development or loss of frost tolerance (as reported in Figure 3). The equations for rT_H, rT_D and rT_S have been formalised in FROSTOL in

agreement with Fowler et al. (1999). The term rT_H (°C d $^{-1}$) is the rate of hardening and it is the only term which is subtracted from the value of the state variable to perform the numerical integration, while the terms rT_D, rT_R and rT_S (°C d $^{-1}$) are added to the state variable value (as reported in Eq. 2).

$$rT_{L50} = -rT_H + rT_D + rT_R + rT_S \quad [2]$$

The rate of hardening decreases T_{L50} and therefore increases frost tolerance. Winter wheat hardening rate has been found to be higher at the start of the acclimation period; this is represented in the model (Eq. 3) by the proportionality between hardening rate and the difference between the frost tolerance already acquired ($T_{L50(t-1)}$, °C) and the maximum frost tolerance that can be realised by the simulated cultivar (T_{L50c}, °C). In agreement with Fowler et al. (1999), a crown temperature (T_c) of 10 °C is assumed as the threshold (T_{i1}) for the initiation of cold acclimation in wheat (i.e. no initiation above 10 °C).

$$rT_H = \begin{cases} c_H \cdot (T_{i1} - T_c) \cdot \left(T_{L50(t-1)} - T_{L50c}\right) & when\ T_c < T_{i1}\ and\ f_V < 0.99 \\ 0 & otherwise \end{cases} \quad [3]$$

Since hardening occurs until the fulfilment of the vernalisation requirement, a variable describing the completion of vernalisation (f_V) is needed. FROSTOL determines the daily rate of vernalisation (Wang and Engel, 1998) and then the accumulated effective vernalisation days (D_V, days). The accumulated vernalisation days are used to estimate the vernalisation response f_V in winter wheat through Eq. 4 (Streck et al., 2003). This quantity is unitless and ranges from 0, before the beginning of the vernalisation process, to 1, at the fulfilment of the vernalisation requirement (as reported in Figure 4).

$$f_V = \frac{(D_V)^5}{[(22.5)^5 + (D_V)^5]} \quad [4]$$

The positive terms rT_D, rT_R and rT_S account for the loss of frost tolerance due to, respectively, dehardening, respiration under a snow cover, and prolonged exposure to near-lethal temperatures. Dehardening rate (rT_D, Eq. 5) has been found to be higher during the first 3 days of exposure at 15 °C, both for non-fully vernalised and fully vernalised winter wheat plants, collected respectively in autumn and spring. The model accounts for this finding through the difference between the T_{L50} of an unacclimated plant (T_{L50i}) and the one reached

by the plant at the previous time step ($T_{L50(t-1)}$). The dehardening rate of non-fully vernalised plants has been found to remain constant after these first three days, while for fully vernalised plants, that did not show the same stabilization, there was a more rapid loss of tolerance. Therefore, after the fulfilment of vernalisation requirements (f_V > 0.99), FROSTOL lowers the temperature threshold for dehardening from 10 °C (T_{i1}) to –4 °C (T_{i2}) and does not allow re-hardening (intended as further hardening after dehardening).

$$rT_D = \begin{cases} c_D \cdot \left(T_{L50i} - T_{L50\,(t-1)}\right) \cdot (T_c + 4)^3 & if\ [f_V < 0.99\ and\ T_c \geq T_{i1}]\ or\ [f_V \geq 0.99\ and\ TC \geq T_{i2}] \\ 0 & otherwise \end{cases} \quad [5]$$

During winter, thick and persistent snow cover allows the soil to remain unfrozen. Plants in unfrozen soils have been reported to have a higher respiration rate than those in frozen soils; moreover, snow cover can lead to anaerobic conditions. Therefore, plants living in an unfrozen soil covered by a snow layer are subject to a loss of frost tolerance, probably due to the accumulation to toxic levels of metabolites deriving from anaerobic respiration, such as CO_2, ethanol and lactate. This accumulation of metabolites increases plant stress causing a loss of frost tolerance. The rate of frost tolerance loss due to respiration under snow cover (rT_R, Eq. 6) is expressed with an empirical equation developed by Bergjord et al. (2008), that includes a respiration factor (f_R, °C, Eq. 7 and Figure 4) and a function of snow depth (f_S, unitless, Eq. 8).

$$rT_R = c_R \cdot f_R \cdot f_S \quad [6]$$

The respiration factor was developed on the basis of respiration measurements, as a function of the crown temperature (Sunde, 1996).

$$f_R = \frac{e^{(0.84 + 0.051 \cdot T_C)} - 2}{1.85} \quad [7]$$

The snow depth function increases linearly from 0 to 1 with snow depth (S, cm) up to a snow depth threshold (S_t = 12.5 cm); for snow depths exceeding this threshold the snow depth function value is constant and equal to 1.

$$f_S = \begin{cases} S\,/S_t & when\ S \leq S_t \\ 1 & when\ S > S_t \end{cases} \quad [8]$$

Finally, since a decrease in winter survival following the exposure to near-lethal temperature has been observed, FROSTOL also calculates a loss of frost tolerance caused by low temperatures (rT_S, Eq. 9). This is accomplished as a function of the difference between the lethal temperature at the previous time step ($T_{L50(t-1)}$), and the temperature to which the crown tissue is exposed.

$$rT_S = \frac{(T_{L50(t-1)} - T_c)}{e^{[-c_S \cdot (T_{L50(t-1)} - T_c) - 3.74]}} \quad [9]$$

5.4.3.2 MODEL BY BYRNS ET AL. (2020)

In the winter survival model by Byrns et al. (2020) the rate variable (rT_{L50}, °C d $^{-1}$) and the numerical integration of the state variable are equal to those previously described for FROSTOL (Eq. 2), as reported in Figure 2.

In Byrns et al. (2020) the initial value of T_{L50} (T_{L50i}) corresponds to -3 °C and represents the T_{L50} of an unacclimated crop. The state variable has an upper limit, which corresponds to the initial value of the state variable itself, and a lower limit, that is represented by the T_{L50} of a fully acclimated plant (T_{L50c}).

The increase of frost tolerance due to hardening (rT_H, Eq. 10) is simulated in the model by Byrns et al. (2020) through a similar approach to the one used by Fowler et al. (1999) in the first version of the winter survival model, which is also the same used in FROSTOL. In contrast to the other models, the hardening rate is equal to zero when the plant is subjected to a loss of frost tolerance due to stressful conditions: respiration under snow cover ($rT_R > 0$, Eq. 17) and exposure to near-lethal temperatures ($rT_S > 0$, Eq. 18). Otherwise, hardening rate is influenced by the vegetative/reproductive transition factor (f_{VRT2}, Eq. 1). This empirical factor describes the development rate from the vegetative to the reproductive growth stage, which is the critical transition that starts the down-regulation of the genes involved in low temperature tolerance and leads to a loss of cold hardiness.

$$rT_H = \begin{cases} 0 & if\ rT_R > 0 \\ \max\left(0, c_H \cdot (T_i - T_c) \cdot \left(T_{L50(t-1)} - T_{L50adj}\right)\right) \times f_{VRT2} & if\ rT_S = 0 \\ 0 & otherwise \end{cases} \quad [10]$$

The value of c_H (0.014 °C^{-1} d^{-1}) used in Eq. 10 is different from the one used in FROSTOL (c_H = 0.0093 °C^{-1} d^{-1}, Eq. 3), since the models are parameterized for different winter wheat cultivars. Since differences in the threshold induction temperature for the start of cold acclimation (hardening) have been observed during a field trial documented by the Authors, and since the expression of genes regulated by low temperatures has been reported for plants exposed to warmer temperatures than those in the induction range, Byrns et al. (2020) used a calculated threshold induction temperature (T_i, °C) for hardening rate, rather than a fixed value (T_{i1}) of 10 °C as in FROSTOL. This threshold induction temperature (Eq. 11) is estimated as a function of T_{L50c}.

$$T_i = 3.72135 - 0.401124 \cdot T_{L50c} \quad [11]$$

In contrast to similar models (FROSTOL, Fowler et al. 1999 and Fowler et al. 2014), Byrns et al. (2020) use T_{L50adj} instead of T_{L50c} for the acclimation rate: T_{L50adj} corresponds to the damage-adjusted T_{L50c} (Eq. 12) and is calculated as the difference between T_{L50c} and the accumulated amount of dehardening due to low temperature and respiration under a snow cover stresses (T_{DS}, Eq. 13).

$$T_{L50adj} = T_{L50c} - T_{DS(t-1)} \quad [12]$$

$$T_{DS(t)} = T_{DS(t-1)} - (rT_R + rT_S) \quad [13]$$

The progress of the crop to the vegetative / reproductive transition (f_{VRT1}, Eq. 14) is described through the fulfilment of three requirements regarding: minimum leaf number (f_{ML}, unitless), vernalisation (f_{VR}, unitless) and photoperiod (f_{PR}, unitless).

$$f_{VRT1} = \min(1, f_{ML}, f_{VR}, f_{PR}) \quad [14]$$

Since f_{ML}, f_{VR} and f_{PR} range between 0 and 1 (as reported in Figure 4), in the model the transition occurs when f_{VRT1} reaches a value of 1. The f_{VRT2} used in Eq. 10 avoids the strict on and off control of hardening and dehardening found in FROSTOL (Eq. 3 and 5), thus allowing the two processes to take place at the same time.

$$f_{VRT2} = \frac{1}{1+e^{80 \cdot (f_{VRT1} - 0.9)}} \quad [15]$$

Also, the formalisation of the loss of frost tolerance due to the dehardening (rT_D, Eq. 16) by Byrns et al. (2020) differs from the models of Fowler et al. (1999) and Bergjord et al. (2008). Indeed the loss of tolerance due to dehardening is calculated using a different approach (Fowler et al., 2014), and depends on crown temperature, T_{L50} and the occurrence of stressful conditions due to respiration under snow cover.

$$rT_D = \begin{cases} \frac{5.05}{1+e^{4.35 - 0.28 \cdot \min(T_c,\ T_i)}} & if\ T_c > T_i\ and\ T_{L50} < T_{L50i} \\ \frac{5.05}{1+e^{4.35 - 0.28 \cdot \min(T_c,\ T_i)}} \cdot (1 - f_{VRT2}) & if\ T_c > T_{L50i}\ and\ T_{L50} < T_{L50i} \\ 0 & if\ rT_R > 0\ or\ else \end{cases} \quad [16]$$

In the model by Byrns et al. (2020), the rate of frost tolerance loss due to plant respiration in unfrozen soils with snow cover (rT_R, Eq. 17) is formalised according to the approach of FROSTOL (Eq. 6 and 7), but the influence of snow depth on the process is not represented in the rate equation through a function as in FROSTOL. Indeed, the loss of frost tolerance due to this type of stress is assumed to start after a deep snow cover that keeps the soil temperature near zero for five days. In the model, these assumptions are implemented in an empirical equation that, using the mean crown temperature of the last five days (T_{cm}) and its standard deviation (T_{csd}), determines snow cover conditions that lead to loss of frost tolerance.

$$rT_R = \begin{cases} c_R \cdot f_R & if\ (T_{cm} < 1.5\ and\ T_{cm} > -1\ and\ T_{csd} < 0.75) \\ 0 & otherwise \end{cases} \quad [17]$$

As in FROSTOL, Byrns et al. (2020) maintained the same approach of Fowler et al. (1999) to estimate the loss of frost tolerance caused by prolonged exposure to near-lethal temperatures (rT_S, Eq. 18). This estimate requires computation of the minimum T_{L50} (T_{L50min}) achieved during the all the previous time steps. This loss is assumed to take place when the following conditions occur simultaneously ($T_{L50} < T_c < T_{L50min}$ and $T_{L50} - T_{DS} < T_{L50i}$ and $T_c < T_{L50i}$), while in every other condition rT_S is equal to 0.

$$rT_S = \left| \frac{T_{L50min} - T_c}{e^{-c_S \cdot (T_{L50min} - T_c)} - 3.74} \right| \quad [18]$$

5.4.3.3 MODEL BY LECOMTE ET AL. (2003)

In the model by Lecomte et al. (2003), the initial value of the state variable (T_R) corresponds to the minimal frost resistance (T_{RN}, °C) measured when hardening has not yet begun. Lecomte et al. (2003) evaluated the frost resistance, prior to hardening, of nine wheat cultivars. Since their observations did not allow them to detect significant differences between wheat cultivars for the minimal frost resistance, they assumed the same T_{RN} value (-6 °C) for all.

The value of the state variable expressing frost resistance (T_R, °C, Eq. 19) depends, as reported in Figure 3, both on the frost resistance acquired at the previous time step ($T_{R(t-1)}$, °C) and on the potential frost resistance that can be obtained during the current time step (T_{RPot}, °C). When $T_{R(t-1)}$ is higher than T_{RPot}, frost resistance (T_R) is assumed to increase. In this situation, hardening (rT_H, °C d^{-1}, Eq. 22 and 23) is simulated. For the opposite situation, when $T_{R(t-1)}$ is lower than $T_{RPot(t)}$, the frost resistance (T_R) is assumed to decrease. In this case, dehardening (rT_D, °C d^{-1}, Eq. 24) is simulated.

$$T_R = \begin{cases} \max\left[\left(T_{R(t-1)} + rT_H\right), T_{RPot}\right] & when\ T_{R(t-1)} > T_{RPot} \\ \min\left[\left(T_{R(t-1)} + rT_D\right), T_{RPot}\right] & when\ T_{R(t-1)} < T_{RPot} \end{cases} \quad [19]$$

The potential frost resistance (T_{RPot}, Eq. 20) depends only on daily mean air temperature (T_a, °C) and ranges from T_{RN} (°C, parameter) to T_{RX} (°C, auxiliary variable, Eq. 21).

$$T_{RPot(t)} = \begin{cases} T_{RN} & when\ T_a \geq 15\ °C \\ T_{RX} + \frac{T_a}{15} \cdot (T_{RN} - T_{RX}) & when\ 0 < T_a < 15\ °C \\ T_{RX} & when\ T_a \leq 0\ °C \end{cases} \quad [20]$$

In the model by Lecomte et al. (2003), the maximal frost resistance is assumed to be genotype dependant and, for a given genotype, is simulated according to the crop phenological stage. The development stage is expressed as leaf stage (N_L, expressed as number of leaves) so that the maximal frost resistance increases linearly from an initial (N_{Li}) to a final leaf stage (N_{Lf}). The simulated leaf stage is estimated on a daily time step; it depends on the cumulated daily mean temperature above zero and the phyllochron. The maximal frost resistance achievable, at each phenological stage, is limited respectively by two parameters: the maximal frost resistance achievable at the coleoptile stage (T_{RX2}, °C) and the one obtainable at the end of the hardening process (T_{RX1}, °C).

$$T_{RX} = \begin{cases} T_{RX2} & if\ N_L < N_{Li} \\ \frac{(T_{RX1} - T_{RX2})}{(N_{Lf} - N_{Li})} \cdot (N_L - N_{Li}) + T_{RX2} & if\ N_{Li} < N_L < N_{Lf} \\ T_{RX1} & if\ N_{Lf} < N_L \end{cases} \quad [21]$$

The authors tested several stage ranges for the increase of the maximal resistance, since they did not agree on the values of N_{Li} and N_{Lf}; the same has been done for the value of the maximal frost resistance at the coleoptile stage (T_{RX2}), while the value of the maximal frost resistance after hardening (T_{RX1}) has been determined, for each genotype, through experimental observations.

For the hardening rate, the authors implemented two different equations (rT_H, Eq. 22 and Eq. 23), which are based on two different hypotheses, assuming a variable or a constant hardening rate, respectively. For both hypotheses, hardening rate is influenced by the daily mean air temperature (T_a) through the estimate of T_{RPot}. Each hypothesis gives rise to a different model configuration.

For the first hypothesis (Eq. 22), hardening rate is proportional to the difference between the potential frost resistance (T_{RPot}) and the frost resistance acquired at the previous time step ($T_{R(t-1)}$). According to this relationship, hardening rate is higher at the beginning of the process (i.e. at the beginning of the hardening period) and lower when frost resistance approaches the maximal frost resistance achieved at the end of the hardening period.

$$rT_H = \left\{1 - e^{\left[\frac{1}{28 + log(0.05)}\right]}\right\} \cdot (T_{RPot(t)} - T_{R(t-1)}) \quad [22]$$

For the second hypothesis (Eq. 23), the constant hardening rate is a function of the difference between the potential frost resistance (T_{RPot}) of the genotype and the minimal frost resistance (*MinR*). The model employing this constant hardening rate was considered by the authors (Lecomte et al., 2003) to be the best performing in a 10-year simulation study.

$$rT_H = \frac{(T_{RPot} - T_{RN})}{28} \quad [23]$$

The dehardening rate (rT_D, Eq. 24) is assumed to be proportional to the daily average air temperature (T_a). Lecomte et al. (2003) do not consider differences, which are difficult to estimate, in dehardening rate and its duration due to genotype, phenological stage, and frost resistance previously acquired ($T_{R(t-1)}$). The authors estimate dehardening rate as a function of the difference between the minimal frost resistance (T_{RN}) and the

maximal frost resistance threshold (T_{RX1}), which corresponds to the negative temperature at which the first leaf necrotic damage occurs. This threshold is genotype-dependent but, differently from T_{RX} which is a function of the leaf stage, it is not dependent on the phenological stage.

$$rT_D = [\frac{T_{RN} - T_{RX1}}{100}] \cdot T_a \quad [24]$$

5.5 MODEL PERFORMANCE

We describe here the results reported in the literature, obtained after calibrating the three models with field data in various sites. FROSTOL was calibrated and then tested, by means of cross validation, using the experimental results derived from a two-year field cold hardiness trial (Bergjord et al., 2008) performed by means of artificial freezing. The trial involved two winter wheat cultivars (Bjørke and Portal) and three sites in Norway (Stjørdal, Selbu, and Oppdal). The sowing dates were September 4, 2003, and September 1, 2004. The three sites differed in their climate: the first one has an oceanic climate, while the other two sites are characterized by lower temperatures and by persistent snow cover during winter months. The authors reported good agreement between measured and simulated T_{L50} values, that ranged between -4 °C (during September) and -23 °C (during November). The root mean square error (RMSE) of T_{L50} for the six combinations of site and year (jointly for the two wheat cultivars) was on average 2.42 °C (with a standard deviation in cross validation of 0.38 °C).

The model by Byrns et al. (2020) is available on-line (https://wheatworkers.ca/wcsm.php) as an interactive tool that allows the user to investigate production risks, breeding and crop management strategies for Canada, Europe, and USA. Tests are available for the two models on which Byrns et al. (2020) based their development (Fowler et al., 1999; Fowler et al., 2014). The model by Fowler et al. (1999) was tested during two winter seasons (1995 and 1996) for the wheat cultivar Norstar in a Canadian site (Saskatoon) that has a warm summer continental climate. Wheat was planted on September 1st and two treatments (seeding on summer fallow and direct seeding in standing stubble) were tested each year. Winterkill events were correctly simulated in both years: the simulated T_{L50} values followed the measured ones (R^2 = 0.96). The model of Fowler et al. (2014) was further tested in Canada between 2003 and 2013 during 12 trials by

collecting 129 T_{L50} values for different cultivars, obtaining a good model performance (RMSE equal to 2.43 °C, Nash-Sutcliffe Model Efficiency equal to 0.88).

Lecomte et al. (2003) tested their algorithms and parameter values for simulating frost resistance to the first frost wave of nine winter wheat cultivars (their T_{RX1} ranged from -12 to -32 °C). They compared simulated and measured frost resistance temperatures (T_R, °C) collected over 10 years (1989-1998) in the field in a site (Chaux-des-Prés, France) that has a temperate oceanic climate. The authors calculated the divergence between simulated and observed frost damage by comparing the simulated frost resistance (°C) with the minimum air temperature recorded when the frost stress occurred. The model configuration that obtained the best agreement between simulated and observed values (i.e. the lowest mean divergence, °C) was the one using: T_{RX2}= -12 °C; N_{Lf} = 3.5 and constant hardening speed (Eq. 24). The mean divergence over 10 years of this model configuration was 0.73 °C (with a standard deviation of 1.20 °C).

5.6 MODEL APPLICATION

5.6.1 METHODOLOGY

The three models designed to simulate winter wheat frost tolerance were implemented in Visual Basic for Applications in Microsoft Excel. To compare the models' behaviour, we applied them in two locations with different climatic conditions (Sant'Angelo Lodigiano, Italy, and Saskaatoon, Canada) with respect to frost tolerance acquisition. For the Italian site, winterkill is not reported in the literature for winter wheat, while it is a more frequent event in the Canadian site (Fowler et al., 1999). A 20-year temperature series (1999-2020) was analyzed to select, for each site, the autumn-winter season whose average value of the minimum daily temperatures of four months (from November to February) was between the fifth and the tenth percentile. The seasons selected for model application are reported in Table 2.

In addition, to underline the key differences among the models, for each location we applied them for a highly frost resistant wheat variety and for a less resistant one (Norstar and Winter Manitou, respectively). We used observed weather data (daily minimum and maximum air temperature and precipitation) and calculated crown temperature and snow depth according to Ritchie (1991). We then ran the three models using the default parameter values (Table A1, A2 and A3), except for the maximal frost resistance which was

assumed to be equal to -24 and to -12 °C for the highly frost resistant variety and for the less resistant one, respectively.

All the simulations started on the first day of September and ended on the first day of May. Crop frost damage was identified for the models by Bergjord et al. (2008) and Byrns et al. (2020) when the average daily soil temperature at the crown level dropped below the simulated lethal temperature T_{L50}, and for the model by Lecomte et al. (2003) when the daily minimum air temperature was equal to or dropped below the simulated frost resistance T_R.

5.6.2 ITALIAN CASE STUDY

Sant'Angelo Lodigiano (45°13' N, 9°24' E, 73 m a.s.l.) is located in the Po plain (northern Italy), where the climate is humid subtropical (Cfa) according to the Köppen classification. For the period September 2005 - April 2006 used in the simulations, the average temperature was 8.7 °C. The temperature of the coldest month (January) was 0.3 °C, and that of the warmest month (September) was 20.3 °C.

None of the models simulated the occurrence of wheat winterkill or frost damage (Figure 5), as the daily average crown temperature and the daily minimum air temperature remained above the simulated T_{L50} and T_R for all the simulation periods. According to FROSTOL and to the model by Byrns et al. (2020), hardening occurred mainly during November, while the model by Lecomte et al. (2003) simulated hardening also until April. Dehardening rates were generally higher than hardening rates, indicating that dehardening was predominant on hardening. Furthermore, in the model by Byrns et al. (2020) and in FROSTOL, dehardening took place mainly from the beginning of January, while the simulations of Lecomte et al. (2003) reported high dehardening rates already during September. The loss of frost tolerance due to respiration under snow cover was simulated only by Byrns et al. (2020), but its extent was negligible. For all the simulations, the maximal frost resistance, corresponding to the minimum value of the state variable, was reached at the end of December / beginning of January (Table 3).

5.6.3 CANADIAN CASE STUDY

Saskatoon (52°07' N, 106° 38' W, 481.5 m a.s.l.) is located in Saskatchewan (Canada) and its Köppen climate classification is warm summer continental climate (Dfb). For the period September 2018 - April 2019 used in

the simulations, the average temperature was -4.9 °C. The temperature of the coldest month (February) was -16.5 °C, and that of the warmest month (September) was 10.4 °C.

In comparison with Sant'Angelo Lodigiano, all models produced relevant hardening rates starting from the first half of September (Figure 6). For all the simulations, maximal frost resistance and the first winterkill event dates are reported in Table 4. For Winter Manitou cultivar (T_{L50c} and T_{RX1} = -12 °C), the model by Byrns et al. (2020) and FROSTOL showed good mutual agreement in the simulated date for winterkill: the former indicated 2007-11-21, the latter 2007-11-26. For this cultivar, the model by Lecomte et al. (2003) indicated the first damage to occur much earlier, on 2007-10-26. The early onset of the simulated damage with this model is caused by the use of the daily minimum air temperature, instead of the crown temperature.

For the Norstar cultivar (T_{L50c} and T_{RX1} = -24 °C), the model by Byrns et al. (2020) simulated a winterkill event (2007-12-06), while in the simulation by FROSTOL the crop survived (no winterkill). A frost damage event was also simulated by the third model (Lecomte et al., 2003) on 2007-11-26. The difference between the simulations of the model by Byrns et al. (2020) and FROSTOL was caused by the different onset of the loss of frost tolerance induced by low temperature stress (that was simulated by Byrns et al. (2020) and was not simulated by FROSTOL) and therefore by the different conditions imposed for this stress in the two models. Low-temperature stress is estimated at each timestep in FROSTOL and it assumes relevance (i. e. its value is greater than zero) when the temperature at which the crown is exposed is lower than the temperature corresponding to the frost resistance acquired at the previous timestep, while in the model by Byrns et al. (2020) low-temperature stress occurs only if several conditions are met (Eq. 18).

5.7 DISCUSSION AND CONCLUSIONS

5.7.1 Similarities and differences among the eight models reviewed

Five (CERES-Wheat, ALFACOLD, FROSTOL, the model by Byrns et al., 2020, and the model by Lecomte et al., 2003) of the eight studied models share a common approach to simulate the dynamics of crop frost tolerance, based on the quantification of frost tolerance acquisition (hardening) and loss (dehardening) in response to crop genotype and environmental conditions. The three winter wheat models (FROSTOL, the model by Byrns et al., 2020, and the model by Lecomte et al., 2003) also consider crop development as a

variable that can affect frost tolerance acquisition. The main difference between these models, apart from the definition of the main model output (see paragraph 4.2.1), is the different number and type of inputs required. The model by Lecomte et al. (2003) requires air temperature, while the other two models require soil temperature in the crown region and other weather inputs such as snow depth for FROSTOL and day length for the model by Byrns et al. (2020).

5.7.2 Differences among the three wheat models

The three models applied in the examples differ for the number of parameters required and for the type and number of processes simulated.

Hardening and dehardening. All models simulate both hardening and dehardening, employing a different number of parameters. Hardening rate is estimated in FROSTOL (Eq. 3) using three parameters (hardening coefficient, maximum frost tolerance of the cultivar, and a cultivar independent threshold induction temperature). The model by Byrns et al. (2020) directly employs (Eq. 10) a hardening coefficient, and four other indirect parameters (three are used to estimate a cultivar-dependent threshold induction temperature, one is used to estimate the damage-adjusted LT_{50}). The model by Lecomte et al. (2003) employs (Eq. 23) two parameters to estimate the constant hardening rate (a cultivar independent minimal frost resistance and a fixed hardening duration). The dehardening rate in FROSTOL (Eq. 5) is formalized using three parameters: a dehardening coefficient and two different cultivar-independent threshold induction temperatures (one used before the fulfilling of the vernalisation requirement, the other one used after), while the model of Byrns et al. (2020) employs directly three empirical parameters for its rate (Eq. 16) and uses indirect parameters involved in the estimation of the cultivar-dependent threshold induction temperature. The model of Lecomte et al. (2003) calculates the dehardening rate (Eq. 24) by means of two explicit parameters (cultivar-dependent maximal frost resistance threshold, minimal frost resistance) and an implicit parameter (i.e. hard-coded). Dehardening estimated by this model showed high variability in the examples, both in the rate values and occurrence, due to its direct dependence on air temperature, while the other two models use soil temperature which has a lower temporal variability.

Effect of stresses on frost tolerance. Compared to the model proposed by Lecomte et al., (2003), FROSTOL and the model by Byrns et al., (2020) differ because they represent two types of stress that cause frost tolerance loss that are not considered by Lecomte et al. (2003): respiration under snow cover, and exposure to low-temperature stress. In both models, the intensity of the stress due to respiration under snow cover is not dependent on cultivar-specific parameters, while the modelling approach of the two models differs on the basis of the input variable (snow depth for FROSTOL and crown temperature for the model by Byrns et al. 2020). It is possible to adopt FROSTOL without measured snow depth values using a snow depth simulation algorithm. Several snow depth models are available, such as the one by Ritchie (1991). Low temperature exposure stress is simulated differently in the two models: in FROSTOL it is simulated at every time-step and its value becomes relevant when the exposure temperature is near the frost tolerance acquired by the plants, while in the model by Byrns et al. (2020) it is estimated only when several conditions are met at the same time. Some of these conditions regard environmental conditions (exposure temperature comprised between the current frost tolerance temperature and the minimum frost tolerance temperature reached during the simulation). Other conditions are involved in the model algorithm (difference between the amount of dehardening due to low temperature stress and current frost tolerance lower than the initial frost tolerance, exposure temperature lower than the initial frost tolerance temperature). For the Italian case study, both types of stress were irrelevant and did not cause significant frost tolerance losses, while low temperature stress was the cause of the sudden frost tolerance loss that led to the winterkill events simulated in the Canadian case study.

5.7.3 Potential for adaptation of these models to cover crops

Some of the reviewed models could be adapted to simulate frost tolerance of frost-sensitive autumn-winter cover crops, thus allowing the assessment of cover crop winterkill for a specific site as a function of crop species and sowing date. Strengths and weaknesses of the three wheat models (FROSTOL, Lecomte et al., 2003; Byrns et al., 2020) are reported in Table 5. Since the occurrence and efficiency of cover crop winterkill is strongly influenced by the development stage reached by the crop at the time of the exposure to sub-zero temperatures, only models considering frost tolerance to be influenced by crop development stage are suitable for this type of application (FROSTOL, Lecomte et al., 2003; Byrns et al., 2020). Attention should be

paid to the fact that FROSTOL and Byrns et al. (2020) simulate the damage at the crown level, while for Lecomte et al. (2003) the level considered is the aerial part of the plants. Furthermore, the output of FROSTOL and Byrns et al. (2020) (lethal temperature for the 50% of the plants) can be practically utilised within a cropping system model to reduce the number of plants and/or of the leaf area of the crop. Therefore, these two models could be suitable to estimate crop overwintering and survival, and the subsequent spring regrowth. FROSTOL can only be applied to species with vernalisation requirements since the development simulation of the model is based on vernalisation, while the models by Byrns et al. (2020) and Lecomte et al. (2003) do not have this restriction, since their development stage is based respectively on the vegetative-reproductive transition factor and on leaf-stage. The simulation of the two types of stress, included both in FROSTOL and in the model by Byrns et al. (2020), can be important for cover crop species, depending on the combination of site, species and sowing/termination dates. Indeed, in the case of late-planted cover crops, that still did not reach their frost tolerance potential at the beginning of the winter season, low temperature stress can lead to winterkill. This type of stress can also cause the winterkill of early-planted cover crops at the end of their growth cycle as they approach flowering, when their frost tolerance decreases due to dehardening. For late-planted cover crops that have meristematic tissues above the ground, the stress imposed by respiration under snow cover could be relevant for frost tolerance, since shorter plants have higher amounts of biomass covered by snow in comparison to taller plants, and therefore be easily damaged. However, this type of stress is less relevant for sites where the snow cover does not significant periods of time.

ALFACOLD provides a simulation of hardening and dehardening for a dicotyledon species, but its application to dicotyledon cover crops could be limited by the lack of consideration given to development stage and by some other model features: the maximum cold tolerance assigned by means of the crop fall growth scores and the lack of the simulation of the first year after crop seeding.

Several current model parameters were obtained by means of calibration against measurements. Adapting the model to cover crops would require careful modification of these parameter values, since three models were developed for wheat and one for alfalfa. The selection of the parameters that should be calibrated to

allow model application to other cultivars and species could be based on global sensitivity analysis of model outputs (Saltelli et al., 2010). Sensitivity analysis should consider several sowing dates in addition to several sites and years used to explore topographic, climatic, and meteorological variability. The calibration of the most sensitive parameters will need to consider the sensitivity to frost of cover crop species, their ability to acquire frost tolerance, and their loss of frost tolerance, through bibliographical sources or experimental trials.

Once calibrated for cover crops, these models will support the simulation of management scenarios in which the susceptibility to 'winterkill' events of cover crops is used in cropping systems to achieve a number of aims. For example, Lorin et al. (2015) have intercropped oilseed rape with winterkilled legume cover crops to achieve weed control, avoiding competition during the cash crop growing season. Storr et al. (2021) have underlined that the terminated cover crop biomass can release nitrogen during its decomposition and, depending on environmental conditions, give rise to undesired nitrate leaching at the end of winter / beginning of spring. Simulation models therefore would be useful in cases like these to evaluate advantages, disadvantages and best application conditions of winterkilled cover crops.

In conclusion, we have shown that the frost damage models by Bergjord et al. (2008), Byrns et al. (2020) and Lecomte et al. (2003) are potentially suitable for simulating cover crop frost damage. We are actively working on this topic and will report calibration results for white mustard in the near future.

ACKNOWLEDGMENTS

We gratefully thank A. K. Bergjord, C. Lecomte and D.B. Fowler who kindly provided details and materials about the equations of their models: FROSTOL (Bergjord et al., 2008), model for frost resistance of wheat (Lecomte et al., 2003), and winter cereal survival model (Byrns et al., 2020).

This work was carried out in the project "Innovazioni per estendere l'uso delle colture di copertura in Lombardia - Innovations to extend the use of cover crops in Lombardy", funded by the Rural Development Programme 2014-2020 of Regione Lombardia, Italy, Operation 16.1.01 (EIP-AGRI Operational Groups).

Weather data were downloaded from Agenzia Regionale per la Protezione dell'Ambiente Lombardia (https://www.arpalombardia.it/Pages/Meteorologia/Richiesta-dati-misurati.aspx for the Italian location) and from the website of the Government of Canada (https://climate.weather.gc.ca/historical_data/search_historic_data_e.html for the Canadian location).

We thank the reviewers for their positive and constructive comments, which helped to improve the manuscript.

References

Ambroise V, Legay S, Guerriero G, Hausman J-F, Cuypers A, Sergeant K, 2020. The Roots of Plant Frost Hardiness and Tolerance. Plant and Cell Physiology 61:3–20.

Barlow KM, Christy BP, O'Leary GJ, Riffkin PA, Nuttall JG, 2015. Simulating the impact of extreme heat and frost events on wheat crop production: A review. Field Crops Research 171:109–119.

Barnes DK, Smith DM, Teuber LR, Peterson MA, McCaslin MH, 1992. Standard tests to characterize alfalfa., Beltsville, MD.

Beck EH, Heim R, Hansen J, 2004. Plant resistance to cold stress: mechanisms and environmental signals triggering frost hardening and dehardening. Journal of biosciences 29:449–459.

Bergjord AK, Bonesmo H, Skjelvåg AO, 2008. Modelling the course of frost tolerance in winter wheat. European Journal of Agronomy 28:321–330.

Brisson N, Launay M, Mary B, Beaudoin B, 2009. Conceptual basis, formalisations and parameterization of the STICS crop model. Éditions Quæ.

Byrns BM, Greer KJ, Fowler DB, 2020. Modeling winter survival in cereals: An interactive tool. Crop Science 60:2408–2419.

Creamer NG, Dabney SM, 2002. Killing cover crops mechanically: Review of recent literature and assessment of new research results. American Journal of Alternative Agriculture 17:32–40.

Fowler DB, Byrns BM, Greer KJ, 2014. Overwinter Low-Temperature Responses of Cereals: Analyses and Simulation. Crop Science 54:2395–2405.

Fowler DB, Limin AE, Ritchie JT, 1999. Low-Temperature Tolerance in Cereals: Model and Genetic Interpretation. Crop Science 39:626–633.

Gusta LV, Fowler DB, 1976. Effects of temperature on dehardening and rehardening of winter cereals. Canadian Journal of Plant Science 56:673–678.

Guy C, 1999. The influence of temperature extremes on gene expression, genomic structure, and the evolution of induced tolerance in plants. Lerner H.R. (Ed.), Plants responses to environmental stresses. from phytohormones to genome reorganization.

Hassan MA, Xiang C, Farooq M, Muhammad N, Yan Z, Hui X, Yuanyuan K, Bruno AK, Lele Z, Jincai L, 2021. Cold Stress in Wheat: Plant Acclimation Responses and Management Strategies. Frontiers in Plant Science 12:676–884.

Janská A, Maršík P, Zelenková S, Ovesná J, 2010. Cold stress and acclimation - what is important for metabolic adjustment? Plant Biology 12:395–405.

Justes E, 2017. Cover Crops for Sustainable Farming. 1st ed. 2017. Springer Netherlands; Imprint: Springer, Dordrecht.

Kanneganti VR, Rotz CA, Walgenbach RP, 1998. Modeling Freezing Injury in Alfalfa to Calculate Forage Yield: I. Model Development and Sensitivity Analysis. Agronomy Journal 90:687–697.

Labreuche J, Bodilis A, 2010. Sensibilite de cultures intermediaires au gel et a l'utilisation de methodes de destruction mecanique. Vingtième et unième conference du columa journées internationals sur la lute contre les mauvaises herbes, 8 et 9 décembre, Dijon.

Labreuche J, Collet A, 2010. Faisabilite de la destruction de cultures intermediaires par le gel ou des moyens mecaniques. Vingtième et unième conference du columa journées internationals sur la lute contre les mauvaises herbes, 8 et 9 décembre, Dijon.

Lecomte C, Giraud A, Aubert V, 2003. Testing a predicting model for frost resistance of winter wheat under natural conditions. Agronomie 23:51–66.

Levitt, J., 1980. 1: Chilling, freezing, and high temperature stresses. Responses of plants to environmental stresses Levitt 1. Academic, New York.

Lorin, M., Jeuffroy, M.-H., Butier, A., Valantin-Morison, M., 2015. Undersowing winter oilseed rape with frost-sensitive legume living mulches to improve weed control. European Journal of Agronomy 71, 96–105. doi:10.1016/j.eja.2015.09.001

McKersie BD, Leshem YY, 1994. Stress and stress coping in cultivated plants. Kluwer academic, Dordrecht.

Muzi C, Camoni L, Visconti S, Aducci P, 2016. Cold stress affects H + -ATPase and phospholipase D activity in Arabidopsis. Plant Physiology and Biochemistry 108:328–336.

Osipitan OA, Dille JA, Assefa Y, Knezevic SZ, 2018. Cover Crop for Early Season Weed Suppression in Crops: Systematic Review and Meta-Analysis. Agronomy Journal 110:2211–2221.

Poeplau C, Don A, 2015. Carbon sequestration in agricultural soils via cultivation of cover crops – A meta-analysis. Agriculture, Ecosystems & Environment 200:33–41.

Ritchie JT, 1991. Wheat phasic development. In: Modeling Plant and Soil System-Agronomy Monograph 31.

Ritchie JT, Otter S, 1985. Description and performance of CERES-Wheat: a user-oriented wheat yield model. ARS wheat yield project 38:159–175.

Saltelli A, Annoni P, Azzini I, Campolongo F, Ratto M, Tarantola S, 2010. Variance based sensitivity analysis of model output. Design and estimator for the total sensitivity index. Computer Physics Communications 181(2):259–270.

Sharpley AN, Williams JR, 1990. EPIC—Erosion/Productivity Impact Calculator: 1. Model Documentation. U.S. Department of Agriculture Technical Bulletin Number 1768.

Smallwood M, Bowles DJ, 2002. Plants in a cold climate. Philosophical Transactions of the Royal Society of London. Series B: Biological Sciences 357:831–847.

Snyder RL, Melo-Abreu JP, 2005. Frost protection: fundamentals, practice and economics. Frost protection 1. Food and Agriculture Organization of The United Nations, Rome.

Storr, T., Simmons, R.W., Hannam, J.A., 2021. Using frost-sensitive cover crops for timely nitrogen mineralization and soil moisture management. Soil Use and Management 37, 427–435. doi:10.1111/sum.12619

Streck NA, Weiss A, Baenziger PS, 2003. A Generalized Vernalization Response Function for Winter Wheat. Agronomy Journal 95:155.

Sunde M, 1996. Effects of winter climate on growth potential, carbohydrate content and cold hardiness of timothy (Phleum pratense L.) and red clover (Trifolium pratense L.). Ph.D. thesis, Agricultural University of Norway, Norway.

Tonitto C, David MB, Drinkwater LE, 2006. Replacing bare fallows with cover crops in fertilizer-intensive cropping systems: A meta-analysis of crop yield and N dynamics. Agriculture, Ecosystems & Environment 112(1):58–72.

Wang E, Engel T, 1998. Simulation of Phenological Development of Wheat Crops. Agricultural Systems 58(1):1–24.

Zheng B, Chenu K, Doherty A, Chapman S, 2015. The APSIM-Wheat Module (7.5 R3008). Available at https://www.apsim.info/wp-content/uploads/2019/09/WheatDocumentation.pdf.

TABLES

Table 1. Selected frost damage models, with state, rate, auxiliary and driving (input) variables. All abbreviations are explained in the text and tables A1 to A3.

Model name	References	State variable	Rate or auxiliary variables	Driving variables
FROSTOL	Bergjord et al. (2008)	lethal temperature 50%	hardening rate; dehardening rate; respiration under a snow cover stress rate; low temperature stress rate	daily average crown temperature; snow depth
(no name)	Byrns et al. (2020)	lethal temperature 50%	hardening rate; dehardening rate; respiration under a snow cover stress rate; low temperature stress rate	daily average crown temperature; daylength
(no name)	Lecomte et al. (2003)	frost resistance temperature	hardening rate; dehardening rate	daily average air temperature
ALFACOLD	Kanneganti et al. (1998)	cold tolerance temperature	hardening rate; dehardening rate	snow depth; daily maximum and minimum air temperature; daylength
CERES-Wheat	Ritchie (1991)	plant density	hardening index	daily average air temperature; snow depth
EPIC	Sharpley and Williams (1990)	biomass	frost damage factor	daily minimum air temperature
APSIM	Zheng et al. (2015)	LAI	frost stress factor	daily minimum air temperature
STICS	Brisson et al. (2009)	plant density; LAI	four frost stress indices, each for a specific phenological phase	daily minimum air temperature

Table 2. Weather conditions in the two sites for model application: crown temperature (simulated), air temperature (measured), snow depth (simulated) and snow cover duration (simulated) for the period September-April.

Site	Year	Crown temperature (10^{th} percentile, °C)	Air temperature (10^{th} percentile, °C)	Snow depth (90^{th} percentile, cm)	Snow cover presence (days)
Sant'Angelo Lodigiano, Italy	2005/2006	+1.54	+0.21	0.00	10
Saskatoon, Canada	2007/2008	-12.12	-21.10	18.80	63

Table 3. Model application example: simulation results for Sant'Angelo Lodigiano (northern Italy), season 2005/2006. T_{L50} is the lethal temperature that kills 50% of the plants, while T_R is the frost tolerance temperature of the crop.

Model	Minimum value of the state variable (T_{L50} and T_R, °C)		Date of attainment of the minimum value		Date of the first winterkill or frost damage event	
	Norstar	Winter Manitou	Norstar	Winter Manitou	Norstar	Winter Manitou
FROSTOL	-22.98	-11.39	2006-01-01	2006-01-01	/	/
Byrns et al. (2020)	-23.99	-11.83	2006-01-01	2006-01-01	/	/
Lecomte et al. (2003)	-24.00	-12.00	2005-12-31	2005-12-31	/	/

Table 4. Model application example: simulation results for Saskatoon (Saskatchewan region of Canada), season 2007/2008. T_{L50} is the lethal temperature that kills 50% of the plants, while T_R is the frost tolerance temperature of the crop.

Model	Minimum value of the state variable (T_{L50} and T_R, °C)		Date of attainment of the minimum value		Date of the first winterkill or frost damage event	
	Norstar	Winter Manitou	Norstar	Winter Manitou	Norstar	Winter Manitou
FROSTOL	-24.00	-11.38	2008-01-29	2007-11-25	/	2007-11-26
Byrns et al. (2020)	-23.82	-10.78	2007-11-10	2007-11-10	2007-12-06	2007-11-21
Lecomte et al. (2003)	-24.00	-12.00	2007-11-19	2007-11-19	2007-11-26	2007-10-26

Table 5. Strengths and weaknesses of the three winter wheat frost damage models.

Model	Strengths	Weaknesses
FROSTOL	1-Output variable (T_{L50}) with clear effect on plant density, suitable for winter survival assessment 2-Easily adaptable to other cereal crops (damage to the crown region) 3-Reduced complexity	1-Calibration with data obtained through artificial freezing test 2-Main driving variable (soil temperature in the crown region) is not commonly measured, but can be simulated 3-Crop development is represented by vernalisation only (therefore the model is not suitable for crops without a vernalisation requirement) 4-Acclimation and de-acclimation processes have respective abrupt ends and starts when vernalisation is completed
Byrns et al. (2020)	1&2 of FROSTOL 3-More complete simulation (compared to FROSTOL) of the vegetative-reproductive transition (vernalisation, photoperiod and minimum leaf number requirements) 4-Smooth transition from acclimation to de-acclimation 5-As opposed to FROSTOL, it does not require snow depth as a driving variable	1&2 of FROSTOL 3-High complexity
Lecomte et al. (2003)	1-Calibration with data obtained in field conditions 2-The driving variable (measured air temperature at 2 m) is easily obtained 3-Easily adaptable to other cereal crops, but also to non-cereal crops (damage is simulated to the above ground biomass) 4-Reduced complexity	1-Frost damage is not quantified by the model (effect on above ground biomass or plant density to be further assessed)

FIGURES

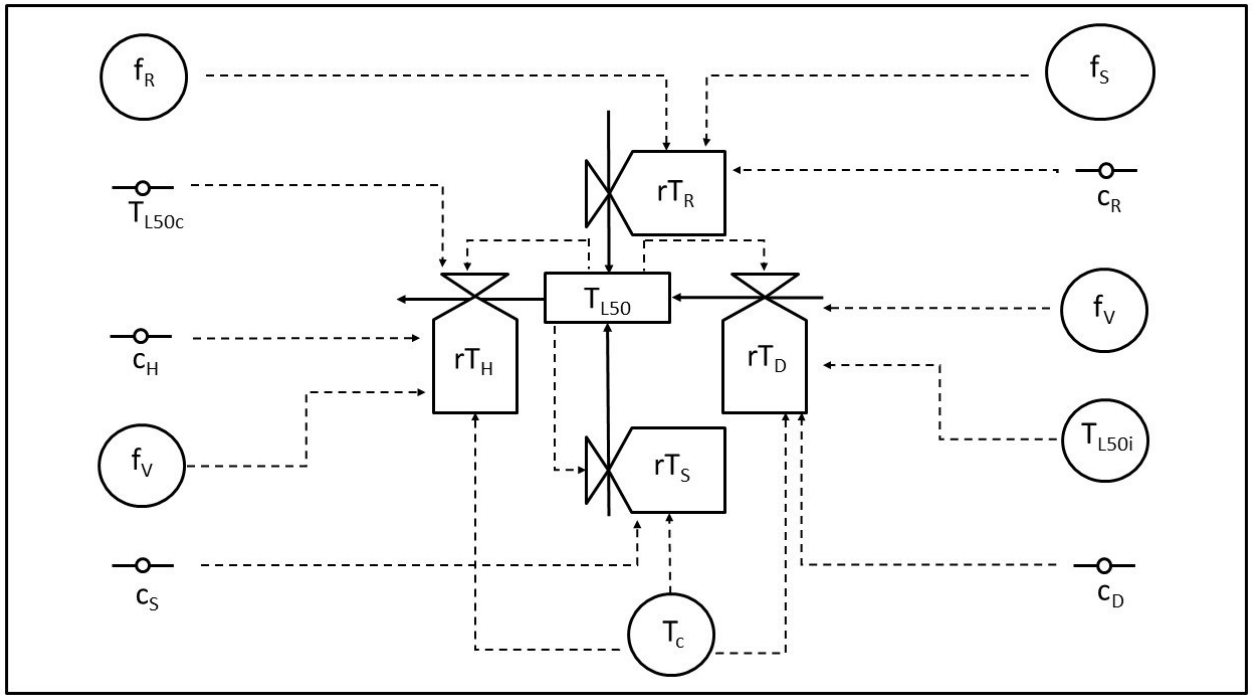

Figure 1. Relational diagram of FROSTOL model by Bergjord et al. (2008). State, rate and auxiliary variables are indicated with a rectangle, a valve symbol and a circle, respectively. Parameters are indicated with a short segment. Continuous lines indicate inputs to and outputs from a state variable. Dotted lines indicate the dependence of a rate or auxiliary variable from a parameter or another variable. The description of model symbols is reported in table A1.

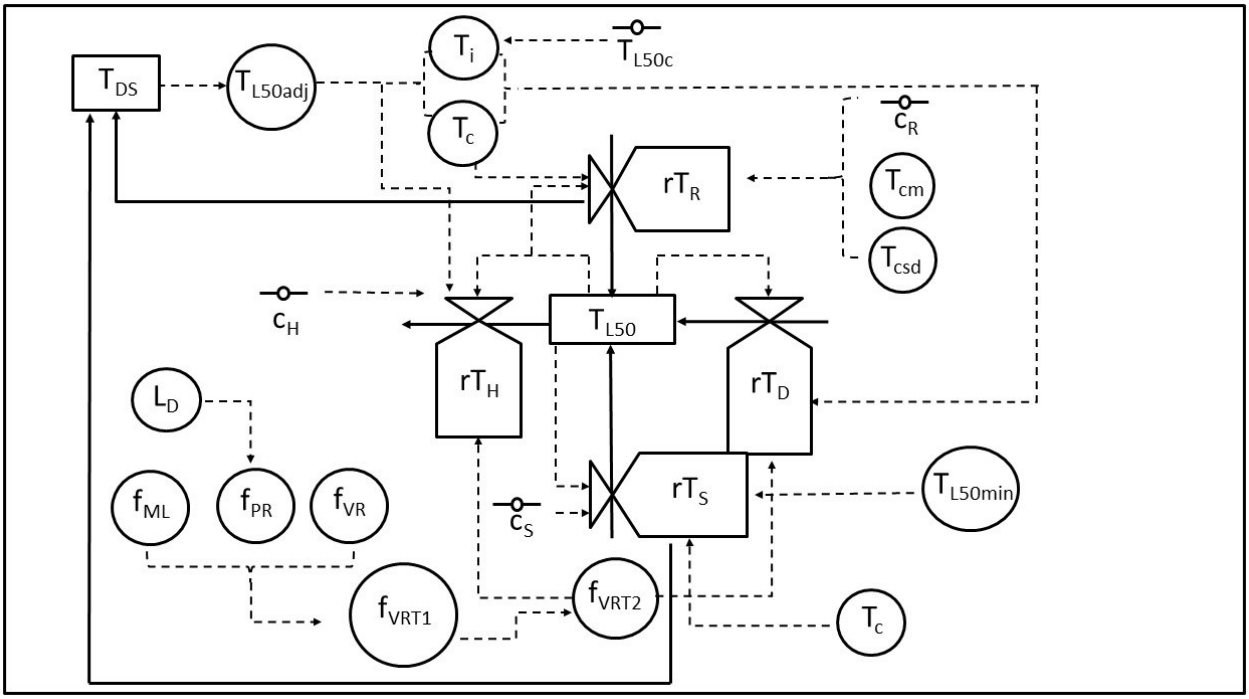

Figure 2. Relational diagram of winter survival model by Byrns et al. (2020). For the explanation of the symbols, see the caption of Figure 1. The description of model symbols is reported in table A2.

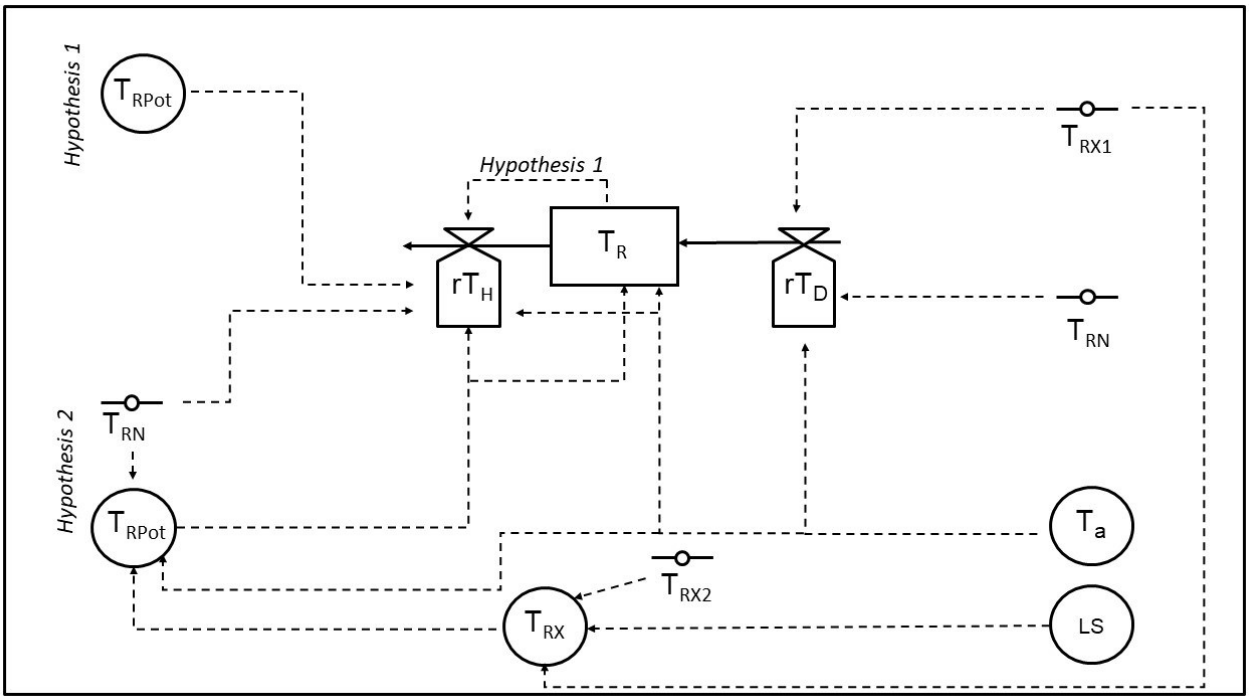

Figure 3. Relational diagram of the model proposed by Lecomte et al. (2003). For the explanation of the symbols, see the caption of Figure 1. The description of model symbols is reported in table A3.

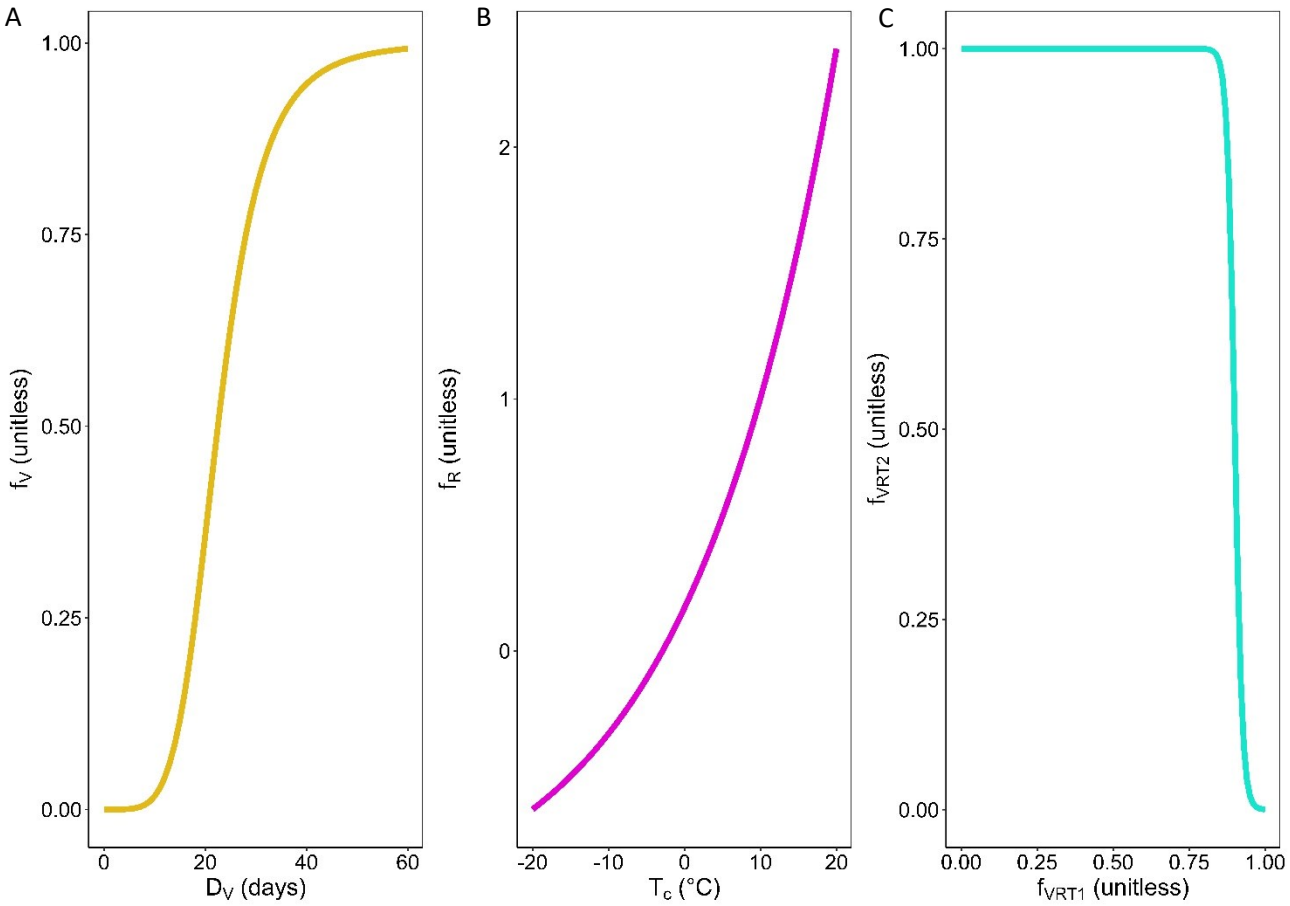

Figure 4. Empirical functions, from the top: A - Vernalisation function (f_V) from FROSTOL model (D_V represents the accumulated vernalisation days); B - Respiration factor (f_R) from FROSTOL and the model by Byrns et al. (2020) (T_c represents daily average crown temperature); C – Vegetative / reproductive transition factor (f_{VRT2}) of the model by Byrns et al. (2020) with f_{VRT1} ranging from 0 (crop sowing) to 1 (flowering stage).

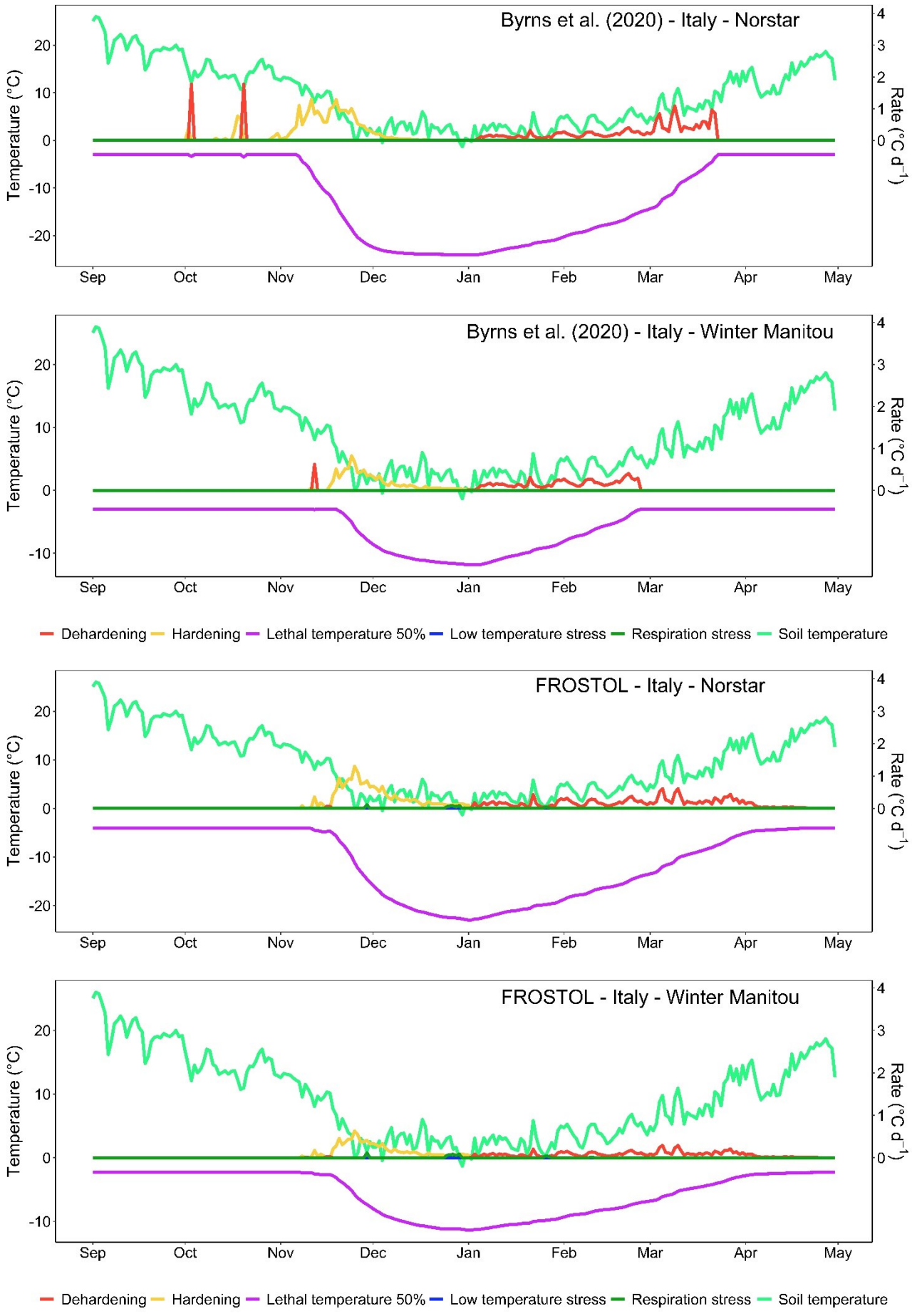
Byrns et al. (2020) - Italy - Norstar
Byrns et al. (2020) - Italy - Winter Manitou
FROSTOL - Italy - Norstar
FROSTOL - Italy - Winter Manitou
Temperature (°C)
Rate (°C d⁻¹)
Sep
Oct
Nov
Dec
Jan
Feb
Mar
Apr
May
Dehardening
Hardening
Lethal temperature 50%
Low temperature stress
Respiration stress
Soil temperature

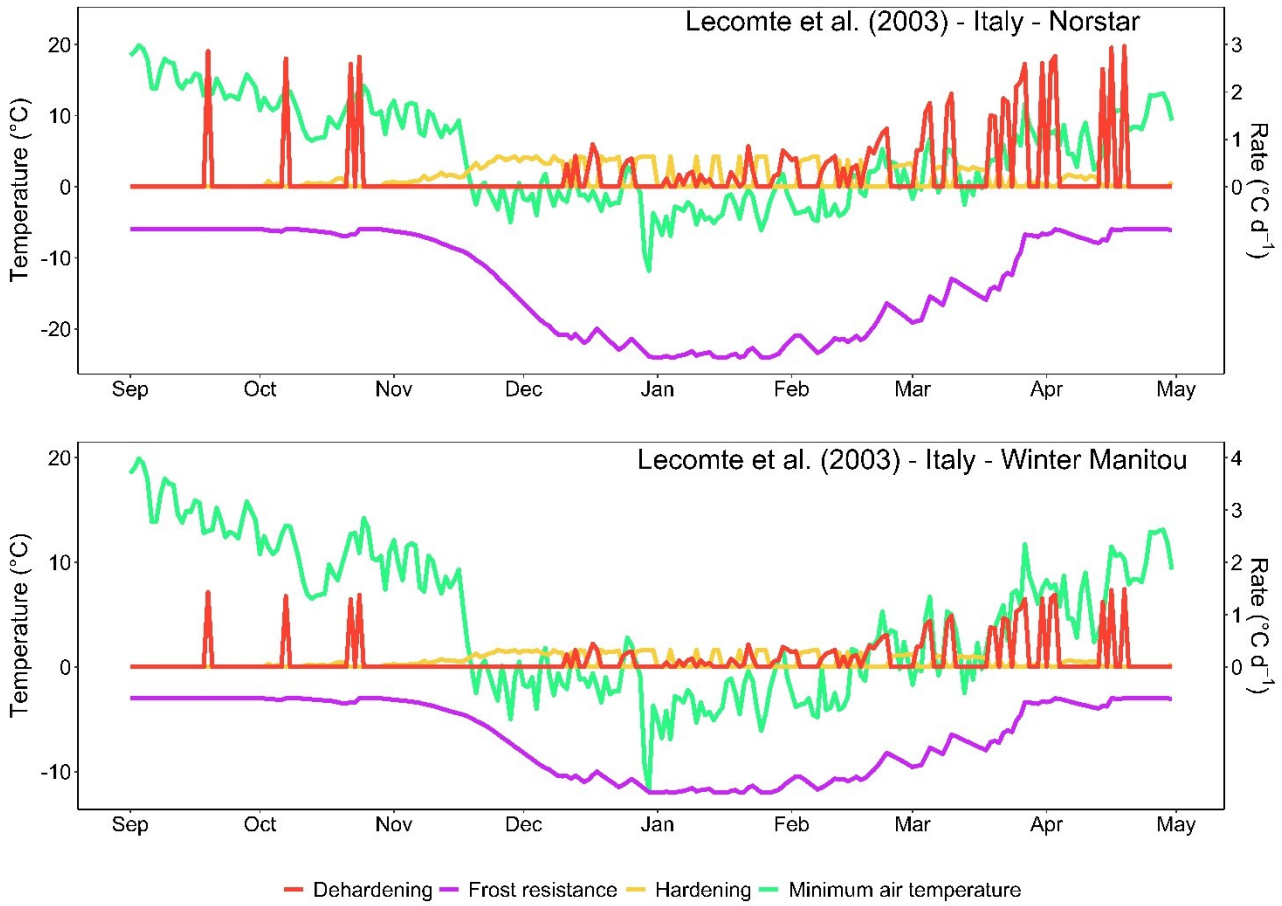

Figure 5. Winter wheat models applied in Sant'Angelo Lodigiano (Italy) for two different winter wheat cultivars: Norstar (plot on the top) and Winter Manitou (plot on the bottom). The scale of all the rate variables (°C d^{-1}) is represented on the right axis. All hardening and dehardening rates are represented in the graphs as positive, even if they act in opposite directions on the value of the state variable.

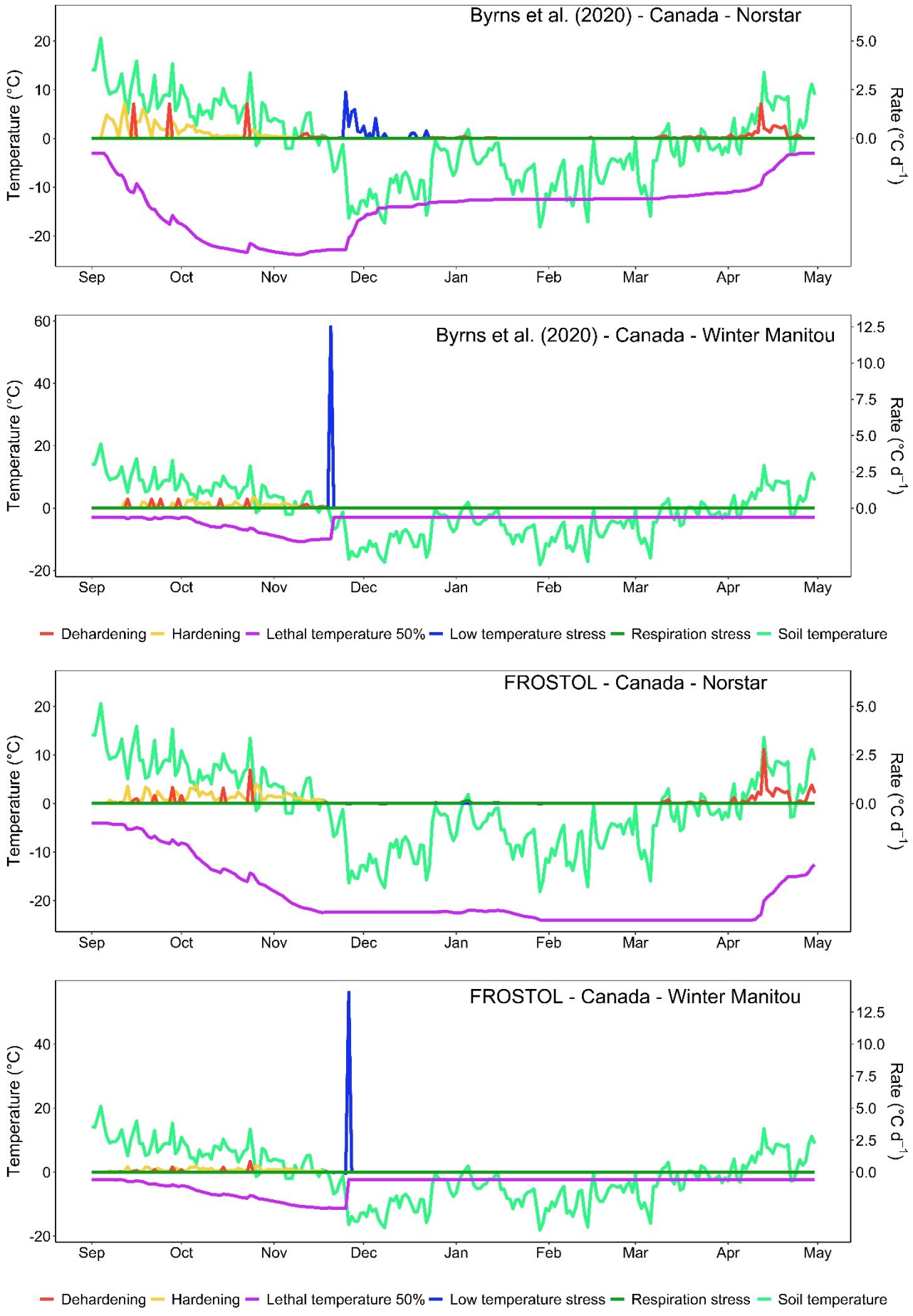
Byrns et al. (2020) - Canada - Norstar
Byrns et al. (2020) - Canada - Winter Manitou
FROSTOL - Canada - Norstar
FROSTOL - Canada - Winter Manitou
Temperature (°C)
Rate (°C d⁻¹)
Sep
Oct
Nov
Dec
Jan
Feb
Mar
Apr
May
Dehardening
Hardening
Lethal temperature 50%
Low temperature stress
Respiration stress
Soil temperature

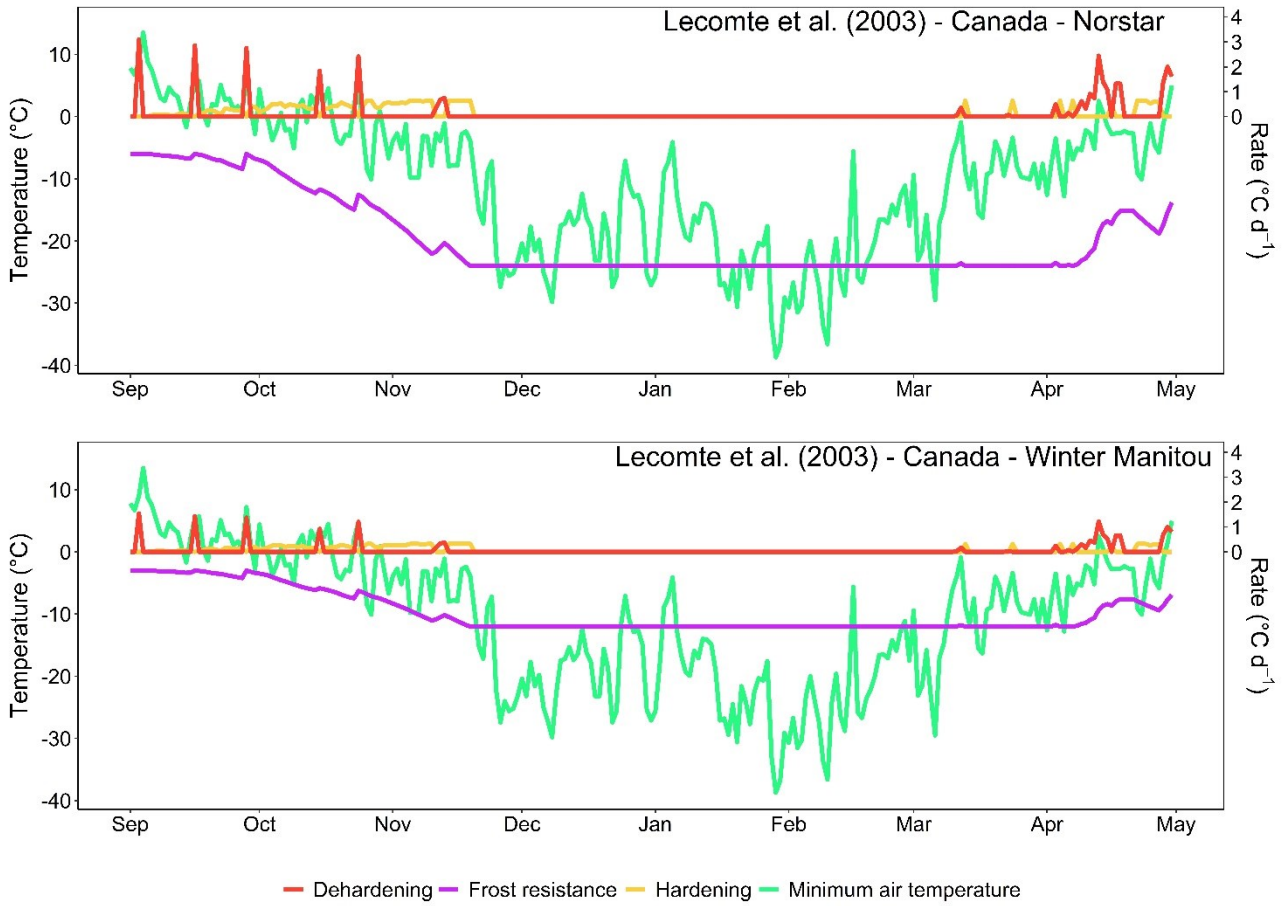

Figure 6. Winter wheat models applied for Saskatoon (Canada) for two different winter wheat cultivars: Norstar (plot on the top) and Winter Manitou (plot on the bottom). The scale of all rate variables (°C d^{-1}) is represented on the right axis. All hardening and dehardening rates are represented in the graphs as positive, even if they act in opposite directions on the value of the state variable.

APPENDIX.

Table A1. Variables and parameters of the model FROSTOL.

Quantity	Type	Units	Description	Default value	Notes
T_{L50}	state variable	°C	lethal temperature for the 50% of the plants		ranges from T_{L50c} to T_{L50i}
rT_H	rate variable	°C d^{-1}	hardening rate		
rT_D	rate variable	°C d^{-1}	dehardening rate		
rT_R	rate variable	°C d^{-1}	respiration under a snow cover stress rate		
rT_S	rate variable	°C d^{-1}	low temperature stress rate		
T_{L50i}	auxiliary variable	°C	T_{L50} initial value		assumed to be constant and cultivar dependent
T_{i1} and T_{i2}	parameter	°C	threshold induction temperature	+10 and -4	assumed to be cultivar independent
f_R	auxiliary variable	°C	respiration factor		
f_S	auxiliary variable	unitless	snow depth function		ranges from 0 to 1
f_V	auxiliary variable	unitless	vernalisation function		ranges from 0 to 1
D_V	auxiliary variable	d	vernalisation days		
T_{L50c}	parameter	°C	maximum frost tolerance of the cultivar		assumed to be constant and cultivar dependent
c_H	parameter	°C d^{-1}	hardening coefficient	0.0093	
c_D	parameter	°C $^{-3}$ d^{-1}	dehardening coefficient	2.7×10^{-5}	
c_R	parameter	d^{-1}	respiration stress coefficient	0.54	
c_S	parameter	°C d^{-1}	low temperature stress coefficient	1.9	

Quantity	Type	Units	Description	Default value	Notes
S_t	parameter	cm	snow depth threshold	12.5	
T_C	driving variable	°C	crown temperature		
S	driving variable	cm	snow depth		

Table A2. Variables and parameters of the model by Byrns et al. (2020).

Quantity	Type	Units	Description	Default value	Notes
T_{L50}	state variable	°C	lethal temperature for the 50% of the plants		ranges from T_{L50c} to $T_{L50\ initial}$
rT_H	rate variable	°C d^{-1}	hardening rate		
rT_D	rate variable	°C d^{-1}	dehardening rate		
rT_R	rate variable	°C d^{-1}	respiration under a snow cover stress rate		estimated through a similar approach to the one of Bergjord et al. (2008)
rT_S	rate variable	°C d^{-1}	low temperature stress rate		estimated through a similar approach to the one of Bergjord et al. (2008)
T_{L50i}	parameter	°C	T_{L50} initial value	-3	assumed to be constant and cultivar dependent
T_i	auxiliary variable	°C	threshold induction temperature		assumed to be constant and cultivar dependent
T_{L50adj}	auxiliary variable	°C	damage-adjusted T_{L50}		
T_{DS}	state variable	°C	amount of dehardening due to low temperature stress		
T_{L50c}	parameter	°C	maximum frost tolerance of the cultivar		assumed to be constant and cultivar dependent
c_H	parameter	°C d^{-1}	hardening coefficient	0.014	
c_R	parameter	d^{-1}	respiration stress coefficient	0.54	
c_S	parameter	°C d^{-1}	low temperature stress coefficient	0.654	
T_{cm}	auxiliary variable	°C	mean crown temperature of the last 5 days		

Quantity	Type	Units	Description	Default value	Notes
T_{csd}	auxiliary variable	°C	standard deviation of the mean crown temperature of the last 5 days		
f_R	auxiliary variable	°C	respiration factor		
f_{VRT1}	auxiliary variable	unitless	progress to the vegetative reproductive transition		ranges from 0 to 1
f_{ML}	auxiliary variable	unitless	minimum leaf number requirement		ranges from 0 to 1
f_{PR}	auxiliary variable	unitless	photoperiod requirement		ranges from 0 to 1
f_{VR}	auxiliary variable	unitless	vernalisation requirement		ranges from 0 to 1
f_{VRT2}	auxiliary variable	unitless	vegetative reproductive transition factor		ranges from 0 to 1
T_C	driving variable	°C	crown temperature		
L_D	driving variable	h	day lenght		

Table A3. Variables and parameters of the model by Lecomte et al. (2003).

Quantity	Type	Units	Description	Default value	Notes
T_R	state variable	°C	crop frost resistance		ranges from T_{RN} (initial value) to T_{RX1}
rT_H	rate variable	°C d^{-1}	hardening rate		
rT_D	rate variable	°C d^{-1}	dehardening rate		ranges from T_{RN} to T_{RX}
T_{RPot}	auxiliary variable	°C	potential resistance acquirable during the current time-step	-6	assumed to be cultivar indipendent
T_{RN}	parameter	°C	minimal frost resistance		depends on genotype and phenological stage
T_{RX}	auxiliary variable	°C	maximal frost resistance		assumed to be constant and cultivar dependent
T_{RX1}	parameter	°C	maximal frost resistance threshold		
T_{RX2}	parameter	°C	maximal frost resistance at coleoptile stage		
T_a	driving variable	°C	average daily air temperature		
N_L	auxiliary variable	n	number of leaves		
N_{Lf}	parameter	n	number of leaves when T_{RX} has its lowest value		
N_{Li}	parameter	n	number of leaves when T_{RX} has its maximum value		

SUPPLEMENTARY MATERIAL.

Table S1. Symbol conversion table

Model	Symbol in this review	Equation number in this review	Symbol in the original paper	Equation in the original paper	Description	Type	Units
FROSTOL	T_{L50}	3; 5 and 9	LT_{50}	2; 3 and 5	lethal temperature for the 50% of the plants	state variable	°C
FROSTOL	rT_H	2 and 3	RATEH	1 and 2	hardening rate	rate variable	°C d^{-1}
FROSTOL	rT_D	2 and 5	RATED	1 and 3	dehardening rate	rate variable	°C d^{-1}
FROSTOL	rT_R	2 and 6	RATER	1 and 4	respiration under a snow cover stress rate	rate variable	°C d^{-1}
FROSTOL	rT_S	2 and 9	RATES	1 and 5	low temperature stress rate	rate variable	°C d^{-1}
FROSTOL	T_{L50i}	1 and 5	LT_{50i}	equations without number	LT_{50} initial value	auxiliary variable	°C
FROSTOL	T_{i1} and T_{i2}	3 and 5	10 and -4	2 and 3	threshold induction temperature	parameter	°C
FROSTOL	f_R	6 and 7	RE	equations without number	respiration factor	auxiliary variable	°C
FROSTOL	f_S	6 and 8	*f*(snow depth)	equations without number	snow depth function	auxiliary variable	unitless
FROSTOL	f_V	3; 4 and 5	*f*(V)	2; 3 and 7	vernalisation function	auxiliary variable	unitless
FROSTOL	D_V	4	VD	7	vernalisation days	auxiliary variable	d
FROSTOL	T_{L50c}	1 and 3	LT_{50c}	2	maximum frost tolerance of the cultivar	parameter	°C
FROSTOL	c_H	3	H_{param}	2	hardening coefficient	parameter	°C d^{-1}
FROSTOL	c_D	5	D_{param}	3	dehardening coefficient	parameter	°C $^{-3}$ d $^{-1}$
FROSTOL	c_R	6	R_{param}	4	respiration stress coefficient	parameter	d^{-1}

Model	Symbol in this review	Equation number in this review	Symbol in the original paper	Equation in the original paper	Description	Type	Units
FROSTOL	c_S	9	S_{param}	5	low temperature stress coefficient	parameter	°C d^{-1}
FROSTOL	S_t	8	T_S_max	4	snow depth threshold	parameter	cm
FROSTOL	T_C	3; 5; 7 and 9	TC	2; 3 and 5	crown temperature	driving variable	°C
FROSTOL	S	8	snowdepth	equation without number	snow depth	driving variable	cm
Byrns et al. (2020)	T_{L50}	10, 16 and 18	LT50	5; 6 and 8	lethal temperature for the 50% of the plants	state variable	°C
Byrns et al. (2020)	rT_H	10	accRate and accFlow	5	hardening rate	rate variable	°C d^{-1}
Byrns et al. (2020)	rT_D	16	dehardRate and dehardFlow	6	dehardening rate	rate variable	°C d^{-1}
Byrns et al. (2020)	rT_R	10; 13; 16 and 17	respFlow	5; 6 and 7	respiration under a snow cover stress rate	rate variable	°C d^{-1}
Byrns et al. (2020)	rT_S	10; 13 and 18	LTstressFlow	5 and 8	low temperature stress rate	rate variable	°C d^{-1}
Byrns et al. (2020)	T_{L50i}	16 and 18	initLT50	6 and 8	LT_{50} initial value	parameter	°C
Byrns et al. (2020)	T_i	10; 11 and 16	thresholdTemp	5 and 6	threshold induction temperature	auxiliary variable	°C
Byrns et al. (2020)	T_{L50adj}	10 and 12	LT50DamageAdj	5	damage-adjusted LT_{50}	auxiliary variable	°C
Byrns et al. (2020)	T_{DS}	12; 13 and 18	dehardAmtStress	8	amount of dehardening due to low temperature stress	state variable	°C
Byrns et al. (2020)	T_{L50c}	11 and 12	LT50c	equations without number	maximum frost tolerance of the cultivar	parameter	°C
Byrns et al. (2020)	c_H	10	no symbol	5	hardening coefficient	parameter	°C d^{-1}
Byrns et al. (2020)	c_R	17	no symbol	7	respiration stress coefficient	parameter	d^{-1}
Byrns et al. (2020)	c_S	18	no symbol	8	low temperature stress coefficient	parameter	°C d^{-1}

Model	Symbol in this review	Equation number in this review	Symbol in the original paper	Equation in the original paper	Description	Type	Units
Byrns et al. (2020)	T_{Cm}	17	fiveDayTempMean	7	mean crown temperature of the last 5 days	auxiliary variable	°C
Byrns et al. (2020)	T_{Csd}	17	fiveDayTempSD	7	standard deviation of the mean crown temperature of the last 5 days	auxiliary variable	°C
Byrns et al. (2020)	f_R	17	no symbol	7	respiration factor	auxiliary variable	°C
Byrns et al. (2020)	f_{VRT1}	14	VRProg	equation without number	progress to the vegetative reproductive transition	auxiliary variable	unitless
Byrns et al. (2020)	f_{ML}	14	mflnFraction	1	minimum leaf number requirement	auxiliary variable	unitless
Byrns et al. (2020)	f_{PR}	14	photoProg	3	photoperiod requirement	auxiliary variable	unitless
Byrns et al. (2020)	f_{VR}	14	vernSaturation	2	vernalisation requirement	auxiliary variable	unitless
Byrns et al. (2020)	f_{VRT2}	10, 15 and 16	VRFactor	4; 5 and 6	vegetative reproductive transition factor	auxiliary variable	unitless
Byrns et al. (2020)	T_C	10; 16 and 18	crownTemp	5; 6 and 8	crown temperature	driving variable	°C
Byrns et al. (2020)	L_D	14	daylength	3	day lenght	driving variable	h
Lecomte et al. (2003)	T_R	19 and 22	R_d	3.1; 5 and 6	crop frost resistance	state variable	°C
Lecomte et al. (2003)	rT_H	19; 22 and 23	dR	3.1; 3.2 and 5	hardening rate	rate variable	°C d^{-1}
Lecomte et al. (2003)	rT_D	19 and 24	dR	4 and 6	dehardening rate	rate variable	°C d^{-1}
Lecomte et al. (2003)	T_{RPot}	19; 20; 22 and 23	$PotR_d$	3.1; 3.2; 5 and 6	potential resistance acquirable during the current time-step	auxiliary variable	°C
Lecomte et al. (2003)	T_{RN}	20; 23 and 24	MinR	3.2 and 4	minimal frost resistance	parameter	°C
Lecomte et al. (2003)	T_{RX}	20 and 21	MaxR	1	maximal frost resistance	auxiliary variable	°C

Model	Symbol in this review	Equation number in this review	Symbol in the original paper	Equation in the original paper	Description	Type	Units
Lecomte et al. (2003)	T_{RX1}	21 and 24	R_s	1 and 4	maximal frost resistance threshold	parameter	°C
Lecomte et al. (2003)	T_{RX2}	21	R_c	1	maximal frost resistance at coleoptile stage	parameter	°C
Lecomte et al. (2003)	T_a	20 and 24	T_m	4	average daily air temperature	driving variable	°C
Lecomte et al. (2003)	N_L	21	LS	1	number of leaves	auxiliary variable	n
Lecomte et al. (2003)	N_{Lf}	21	fLS	1	number of leaves when T_{RX} has its lowest value	parameter	n
Lecomte et al. (2003)	N_{Li}	21	iLS	1	number of leaves when T_{RX} has its maximum value	parameter	n

S1. ALFACOLD

The state variable in ALFACOLD (*CTT*) is initialized to 0 °C; its minimum value is limited by the auxiliary variable *CTMX* (°C), which is the maximum cold tolerance being the lowest subzero temperature that a cultivar can tolerate without being killed. Kanneganti et al. (1998) used a single initial value of cold tolerance temperature (*CTT* = 0 °C) for alfalfa cold-hardy, cold-sensitive and non-hardy cultivars, while the genetic potential for maximum cold tolerance (*CTMX*) differs between the abovementioned types of cultivars as a function of a fall growth score (*FGS*, a standard scale for describing alfalfa cultivar's potential for dormancy and cold tolerance (Barnes et al., 1992).

The net increase or decrease of frost tolerance (Eq. S1.1) is expressed as the difference between the daily rate of hardening (*HRI*, °C d^{-1}) and the daily rate of dehardening (*HRD*, °C d^{-1}).

$$\frac{\Delta CTT}{\Delta t} = (HRI - HRD) \quad \text{[S1.1]}$$

The daily rate of increase in cold tolerance due to hardening (*HRI*, °C d^{-1}), Eq. S1.2, is directly proportional to the maximum rate of hardening (*CHRMX*, °C d^{-1}), which represents the influence of genotype on frost tolerance acquisition, and to a rate modifier (*ETDRI*, unitless) that, being a function of the average daily crown temperature (*CRTMP*, °C), represents its effect on the maximum hardening rate.

$$HRI = CHRMX \times ETDRI \quad \text{[S1.2]}$$

Hardening starts when crown temperature (*CRTMP*) is lower than 15 °C (indeed when crown temperature is lower than 15 °C *ETDRI* ranges from 0 to 1, while when the crown temperature is higher than 15 °C *ETDRI* ranges from 0 to -1) and continues at its maximum rate (*CHRMX*) when crown temperature drops below 10 °C. That is represented in the model by means of the rate modifier *ETDRI* (Eq. S1.3).

$$ETDRI = \begin{cases} 1 & when\ CRTMP \leq 10 \\ -\frac{1}{5} \times CRTMP + 3 & when\ 10 < CRTMP \leq 20 \\ -1 & when\ CRTMP > 20 \end{cases} \quad \text{[S1.3]}$$

One difference between this and the other models is that the reversal of hardening, which occurs when crown temperature is warmer than 15 °C, is modeled separately from dehardening by assigning negative values to *ETDRI* (from 0 to –1) when crown temperature is higher than 15 °C. Kanneganti et al. (1998) adopted

this approach because the reversal of hardening, which occurs during autumn and early winter, has been found to be much slower than dehardening that occurs at similar temperatures during spring.

The dehardening process, in contrast to Bergjord et al. (2008) and Fowler et al. (2014), is simulated for the period of time during which the daylength (*DL*, h) increases, since the photoperiod has been reported to induce metabolic changes related to the start of dehardening.

The daily rate of dehardening (*HRD*, °C d^{-1}) is formalised (Eq. S1.4) through the use of a maximum dehardening rate (*CDRMX*, °C d^{-1}) expressing the genetic control on the process and through a rate modifier (*ETDRB*, unitless).

$$HRD = \begin{cases} CDRMX \times ETDRB & if\ (DL_t - DL_{t-1}) > 0 \\ 0 & if\ (DL_t - DL_{t-1}) \leq 0 \end{cases} \quad [S1.4]$$

The rate modifier *ETDRB* (Eq. S1.5) represents the effect of average daily crown temperature: *ETDRB* is zero for crown temperatures below 0 °C (meaning that no dehardening occurs), while it increases from zero to one as crown temperature rises from 0 to 5 °C; for temperatures above 5 °C its value is constant and set to one (meaning that dehardening occurs at its maximum rate).

$$ETDRB = \begin{cases} 0 & when\ CRTMP \leq 0 \\ \frac{1}{5} \times CRTMP & when\ 0 < CRTMP < 5 \\ 1 & when\ CRTMP \geq 5 \end{cases} \quad [S1.5]$$

ALFACOLD estimates the average daily soil temperature in the crown region at 3 cm depth (*CRTMP*, °C) through Ritchie's (Ritchie, 1991) model (Eq. S1.6 and S1.7). The average daily crown temperature is obtained averaging the estimates of the daily maximum (*CRTMX*, °C) and minimum (*CRTMN*, °C) crown temperatures. The maximum and minimum crown temperatures are calculated as functions of daily maximum (*TMX*, °C) and minimum (*TMN*, °C) air temperatures and of snow depth (*DS*, cm).

$$\mathrm{CRTMX} = \begin{cases} 2 + TMX \times [0.4 + 0.0018 \times (DS - 15)^2] & if\ TMX < 0 \\ TMX & if\ TMX \geq 0 \end{cases} \quad [S1.6]$$

$$\mathrm{CRTMN} = \begin{cases} 2 + TMN \times [0.4 + 0.0018 \times (DS - 15)^2] & if\ TMN < 0 \\ TMN & if\ TMN \geq 0 \end{cases} \quad [S1.7]$$

Plant mortality due to freezing injury is estimated by ALFACOLD through a crop death coefficient (PDF, d^{-1}), which quantifies the fraction of a crop, described as plant density, that die when the crown temperature (*CRTMP*) drops below the cold tolerance temperature (*CTT*). When the crown temperature is warmer than the cold tolerance temperature no freezing injury is simulated since PDF = 0. For each cultivar, the authors determined a potential rate of plant death (*PDFMX*, $d^{-1}°C^{-1}$ below *CTT*), therefore the model estimates (Eq. S1.8) plant death at a cultivar-specific rate and in proportion to plant current stare of cold tolerance.

$$PDF = PDFMX \times max(0, CTT - CRTMP) \quad \text{[S1.8]}$$

S2. CERES-WHEAT

Frost tolerance is simulated by CERES-Wheat through a hardening index (*HI*, unitless) based on the concepts by Gusta and Fowler (1976). This hardening index is used to determine, on a daily basis, the temperature at which the plants are killed by frost. A winterkill function is then applied between emergence and anthesis; if the conditions are met, this leads to the death of 100% of the plants. The hardening index (*HI*, unitless) ranges from 0 to 2 (fully hardened plant). Its value (Eq. S2.9) is increased by hardening and decreased by dehardening (Ritchie, 1991).

$$HI_t = HI_{t-1} + (dH - dD) \times t \quad \text{[S2.9]}$$

The crown temperature average (T_{cr}, °C) and maximum (T_{cr_max}, °C) values are calculated as in ALFACOLD model. Hardening (Eq. S2.10) is assumed to take place in two crown temperature ranges: the first one is referred to the first phase of hardening (that is completed after 10 days of exposure to this temperature range), the second one is referred to the second phase of hardening (completed in 12 days of exposure). Hardening is also assumed to occur, during the first phase, at temperatures above the indicated range: in this case the hardening increment is calculated proportionally. At the end of the first hardening phase the hardening index is equal to 1, while at the end of the second hardening phase the hardening index is equal to 2.

$$dH = \begin{cases} 0.1 & if\ HI < 1\ and - 1 \leq T_{cr} \leq 8 \\ 0.083 & if\ HI > 1\ and\ T_{cr} \leq 0 \end{cases} \quad \text{[S2.10]}$$

The daily decrement of the hardening index due to dehardening process is a function of the maximum crown temperature. The dehardening decrement (Eq. S2.11) is higher during the first hardening phase and lower during the second one.

$$dD = \begin{cases} 0.04 \times (T_{cr\_max} - 10) & if\ HI < 1\ and\ T_{cr\_max} > 10 \\ 0.02 \times (T_{cr\_max} - 10) & if\ HI > 1\ and\ T_{cr\_max} > 10 \end{cases} \quad [S2.11]$$

The hardening index is used to estimate a threshold killing temperature (T_k, °C) through a fixed function (Eq. S2.12). The author (Ritchie, 1991) assumes that when the difference between the average daily crown temperature and the threshold killing temperature is higher than 7 °C at least the 95% of the plants are subject to a winterkill event.

$$T_k = -6 \times (1 - HI) \quad [S2.12]$$

S3. EPIC

EPIC computes, with a daily time step, a multiplicative stress factor which is then used to reduce the standing live biomass (B_{AG}). A unique formalisation of the stress factor is adopted for the entire simulation of the crop cycle. The stress factor is named frost damage factor *FRST* (unitless). The resulting frost damage is greater for early growth stages and tends to 0 for the final development stages (Sharpley and Williams, 1990).

The frost damage factor is a function of the minimum daily air temperature (T_{mn}, °C) that includes two parameters ($af_{j,1}$ and $af_{j,2}$) to define crop frost sensitivity. The frost damage factor (Eq. S3.13) is estimated for dormant fall planted crops when the minimum temperature is below -1 °C (Sharpley and Williams, 1990).

$$FRST_i = \frac{-T_{mn,i}}{-T_{mn,i} - \exp(af_{j,1} + af_{j,2} \times T_{mn,i})} \quad [S3.13]$$

The crop biomass reduction (ΔB_{AG}, t ha^{-1}) during the dormant winter period is then estimated (Eq. S3.14) by the authors (Sharpley and Williams, 1990) as a function of the frost damage factor, a heat unit index (*HUI*, unitless) and a day length reduction factor (*FHR*, unitless).

$$\Delta B_{AG,i} = 0.5 \times B_{AG,i} \times (1 - HUI_i) \times \max(FRH_i, FRST_i) \quad [S3.14]$$

S4. APSIM

Similarly to EPIC, APSIM computes, with a daily time step, a multiplicative stress factor that is used to reduce the leaf area index (*LAI*) for the entire simulation of the crop cycle. The stress factor ($k_{sen,\ frost}$, unitless) is used to estimate the leaf area senescence due to frost ($\Delta LAI_{sen,\ frost}$, unitless, Eq. S4.15). Its value is obtained through linear interpolation using a function of the daily minimum air temperature that is defined by two parameters, currently its default value is set to zero meaning that frost stress is not taken into account in this version of APSIM wheat growth model (Zheng et al., 2015).

$$\Delta LAI_{sen,frost} = K_{sen,frost} \times LAI \quad \text{[S4.15]}$$

In addition to leaf senescence due to leaf aging ($\Delta LAI_{sen,\ age}$) and due to shading ($\Delta LAI_{sen,\ light}$), the daily total leaf area senescence (ΔLAI_{sen}, Eq. S4.16) is estimated considering: frost ($\Delta LAI_{sen,\ frost}$), heat ($\Delta LAI_{sen,\ heat}$) and water ($\Delta LAI_{sen,\ sw}$) stress.

$$\Delta LAI_{sen} = \max(\Delta \mathrm{LAI}_{sen,\ age}, \Delta \mathrm{LAI}_{sen,\ light}, \Delta \mathrm{LAI}_{sen,\ frost}, \Delta \mathrm{LAI}_{sen,\ heat}, \Delta \mathrm{LAI}_{sen,\ sw}) \quad \text{[S4.16]}$$

S5. STICS

The multiplicative stress factor approach used by STICS differs from EPIC and APSIM due to the number of different stress factors calculated: STICS employs four different functions to obtain four frost stress indices (*FGELLEV*, *FGELJUV*, *FGELVEG*, *FGELFLO*). Each stress index is calculated for a specific phenological phase and acts proportionally on a different growth state variable. The response to the temperature and therefore the entity of frost damage depends on the development stage of the crop. These frost stress indices range between 1 (no frost damage) and 0 (lethal frost). *FGELLEV* is computed for the plantlet phase and reduces plant density; *FGELJUV* and *FGELVEG* are calculated for juvenile phase and for post-juvenile phase, respectively, and they both accelerate leaf area senescence. The last one, *FGELFLO*, concerns the reproductive phase which is not of interest for this review.

The four stress indices (*FGELLEV*, *FGELJUV*, *FGELVEG*, *FGELFLO*) are calculated as functions of minimal crop temperature (*TCULTMIN*, °C) that can obtained through empirical approach or energy balance. Each stress

function is defined by four parameters representing *TCULTMIN* values (Brisson et al., 2009). Two parameters, the temperature at the beginning of frost action, (*TDEBGEL*$_P$, 0 °C) and lethal temperature (*TLETALE*$_P$, -13 °C) are independent of phenological stage; while the others are stage-dependent (temperatures corresponding to 10%, *TGEL10*$_P$, and 90% frost damage, *TGEL90*$_P$) therefore these parameters assume different values in different phenological stages. The stress functions, which are split linear functions, are reported by the authors (Brisson et al., 2009) in graphical form.

Plant density reduction due to frost damage (Eq. S5.17) is represented by multiplying the plant density at emergence (*DENSITE(ILEV)*, plant m^{-2}) by the stress index of the plantlet phase (*FGELLEV(I)*, unitless).

$$DENSITE(I) = DENSITE(ILEV) \times FGELLEV(I) \quad \text{[S5.17]}$$

To determine the leaf death acceleration due to stress factor (*SENSTRESS*, unitless), the frost stress indices *FGELJUV* and *FGELVEG* (indicated both as *FSTRESSGEL* in Eq. S5.18) are compared with other two stress indices: the water stress (*SENFAC*, unitless) and the nitrogen stress indices (*INNSENES*, unitless) that are both active on leaf death.

$$SENSTRESS(J) = \min\left(SENFAC(J), INNSENES(J), FSTRESSGEL(J)\right) \quad \text{[S5.18]}$$